

III-4

Surface,
Interface and
Thin Films

BL6U

Anomalous Interfacial Interaction at Polycyclic Aromatic Hydrocarbon Monolayers on Graphene Layer

H. Yamane and N. Kosugi

Institute for Molecular Science, Okazaki 444-8585, Japan

Two-dimensional sp^2 carbon layer, graphene, has a honeycomb network, which induces unique low-dimensional electronic properties such as an in-plane high carrier mobility (ca. 15,000 cm^2/Vs at 300 K). The ABAB-stacking graphene multilayer shows the electronic structure of the single-crystalline graphite. As the graphene sheet can be obtained simply by multiple peeling of graphite with the sticky tape, the interlayer (out-of-plane) interaction in graphite is dominated by the weak π - π interaction. Therefore, organic/graphite interfaces have been regarded as an archetypal model system for electronic and structural studies of physisorbed organic molecules. On the other hand, hexa-*peri*-hexabenzocoronene [HBC, see inset of Fig. 1(b)] is a molecular unit graphene. In the present work, we have succeeded to observe the anomalous interfacial interaction in the HBC monolayers on graphene and graphite by angle-resolved photoemission spectroscopy (ARPES).

The present experiment was performed at BL6U. The photon energy ($h\nu$) for ARPES was 50 eV, which can probe $k_z = na_z^*$ for graphite. The single layer graphene (SLG) and the single crystalline graphite (SCG) were grown on a 6H-SiC(0001) substrate by annealing at 1150°C under the Si flux and 1600°C, respectively [1]. The surface crystallinity of SLG and SCG was characterized using low-energy electron diffraction (LEED) and ARPES.

Figure 1 shows the LEED image and ARPES (E - k_{\parallel}) map around the K point in the Γ -K direction for (a) HBC/SLG and (b) HBC/SCG at 20 K. The LEED images indicate the $p(\sqrt{31}\times\sqrt{31})R9.0$ ordered structure for both interfaces. The E - k_{\parallel} map shows a well-known π -band dispersion of graphene and graphite (π_{Gr}) around the K point. The highest occupied molecular orbital (HOMO)-derived peak of HBC appears at different binding energy (E_b) position depending on the substrate; $E_b = 2.1$ eV for HBC/SLG and $E_b = 1.8$ eV for HBC/SCG. The charge transfer from SiC through the graphene layer might exist at HBC/SLG.

It is of note that the HOMO-derived peak shows a dispersion for both interfaces, which does not depend on the graphene layer thickness. As shown in Fig.2(a), the HOMO-derived peak at HBC/SCG disperses to the lower- E_b side with increasing k_{\parallel} from 1.56 \AA^{-1} to 1.86 \AA^{-1} . The total dispersion width is 105 meV. Furthermore, the HOMO-derived peak involves the vibrational satellites at the higher- E_b side, which also show the dispersive behavior with respect to the 0-0 transition peak, as shown in Fig. 2(b). The observed evidence suggests that the upper (bottom) HOMO band with the anti-bonding (bonding) character around

$k_{\parallel} = 1.82$ \AA^{-1} (1.58 \AA^{-1}) can effectively couple with high (low) frequency phonons.

Since such dispersive behaviors for HOMO and its vibrational satellites are not observable for iron-phthalocyanine/SLG [2] and HBC/Au(111) [3], the molecule-substrate interfacial π - π coupling can play a crucial role in the MO delocalization.

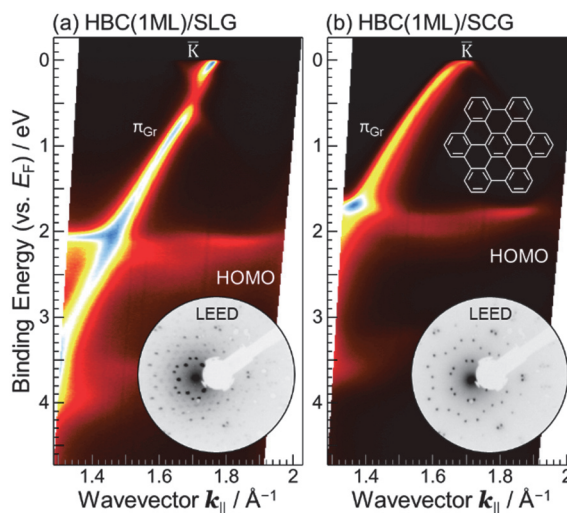


Fig. 1. LEED image and ARPES (E - k_{\parallel}) map around the K point in the Γ -K direction for (a) HBC/SLG and (b) HBC/SCG, measured at $h\nu = 50$ eV and $T = 20$ K.

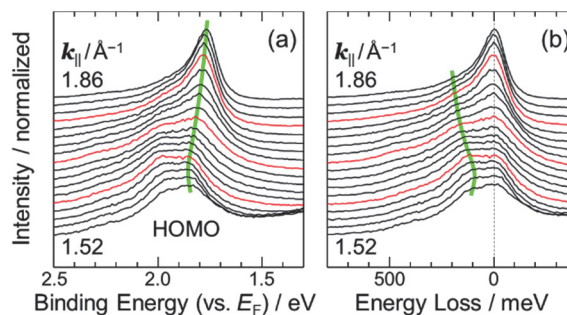


Fig. 2. Energy distribution curves for the HOMO region at HBC/SCG with the k_{\parallel} step of 0.02 \AA^{-1} , wherein the energy scale is measured from (a) the Fermi level and (b) the 0-0 transition peak.

[1] I. Forbeaux, J.-M. Themlin and J.-M. Debever, Phys. Rev. B **58** (1998) 16396.

[2] M. Scardamaglia *et al.*, J. Phys. Chem. C **117** (2013) 3019.

[3] H. Yamane and N. Kosugi, to be published.

BL2B

ARUPS of DNTT on a-TES Film Prepared on Copper Oxide

K. K. Okudaira and S. Nomoto

Graduate School of Science and Engineering, Chiba University, Chiba 263-8522, Japan

An organic thin-film transistor (OTFT) is likely to have suitable applications requiring large-area coverage, structural flexibility and low-cost. However, there are still many issues such as low mobility to be addressed for practical organic electronics. To achieve high mobility it is important to improve the charge injection efficiency at the interface between the metal electrode and the organic semiconductor layer and charge transfer probability. Self-assembled monolayers (SAMs) has been introduced on metal electrode in order to modify the work function of the metal [1].

A triazine-based molecular adhesion agent (a-TES : 6-triethoxysilyl propylamino-1,3,5- triazine- 2,4-dithiol (TES)) was used for preparing thin film like self- assembly monolayers on metal surface as well as SiO₂ insulator layer.

In this work we used a-TES modified copper oxide substrate and examined the molecular orientation of dinaphtho[2,3-b:2',3'-f]thieno[3,2-b]thiophene (DNTT) thin films thermally deposited on the surface by angle- resolved ultraviolet photoelectron spectroscopy (ARUPS) measurements. To obtain the quantitative analysis on the molecular orientation; we compare observed take-off angle dependence of π band and calculated ones by the independent-atomic-center (IAC)/ MO approximation [2].

ARUPS measurements were performed at the BL2B of the UVSOR. The take-off angle (θ) dependencies of photoelectron spectra were measured with the photon energy ($h\nu$) of 28 eV. We use a-TES modified copper oxide (CuO) and CuO as substrate. Copper substrate was subjected to ultrasonic cleaning for 10 minutes in acetone, isopropanol, and then ozone cleaning for 30 minutes. a-TES modified CuO substrate was obtained by dipped in 0.1% solution at 20 °C for 30 minutes. DNTT was deposited on 1.5 nm on both substrates.

We observed take-off angle (θ) dependence of HOMO peak in UPS of DNTT deposited on CuO and a-TES/(CuO) and (thickness of 1.5 nm).

The HOMO peaks of DNTT on CuO and on a-TES/C appear at binding energy of about 1.2 eV and 1.5eV, respectively. The HOMO peaks of DNTT both on SiO₂ and on a-TES/SiO₂ show intense peaks at higher take- off angle ($\theta = 60^\circ$), and at lower θ these intensities become small. For DNTT/CuO, HOMO intensity at $\theta = 38^\circ$ (about 40°) is almost same as that at $\theta = 60^\circ$. On the other hand, for DNTT/a-TES/CuO, HOMO intensity at $\theta = 40^\circ$ is smaller than that at $\theta = 60^\circ$. Due to the difference of θ dependence of HOMO peak of DNTT on CuO and on a-TES/CuO, it is found that the molecular orientation of DNTT on CuO is different from that on a-TES/CuO. The difference of

surface energy of a-TES and CuO indicates that the surface modification by a-TES affects the molecular orientation of organic semiconductor layer, which would have an effect on the characteristics of OTFT such as mobility.

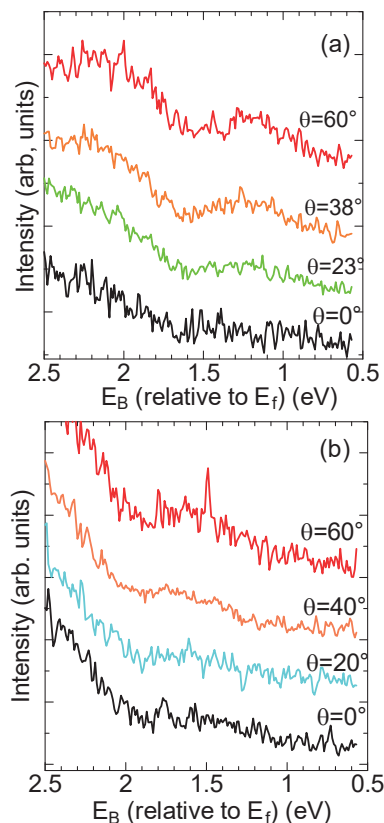


Fig. 1. ARUPS of DNTT(1.5nm)/CuO (a) and DNTT(1.5nm)/a-TES/CuO (b).

- [1] F. Wang *et al.*, *Nanoscale Res. Lett.* **6** (2011) 483.
 J. -P. Hong *et al.*, *Appl. Phys. Lett.* **92** (2008) 143311.
 [2] N. Ueno *et al.*, *J. Chem. Phys.* **99** (1993) 7169.

BL2B

Phase Stability of Quasi-1 Dimensional Columnar Structure of Tin-phthalocyanine Films

Y. Kashimoto¹, H. Ichikawa¹ and H. Yoshida^{1,2}

¹ Graduate School of Engineering, Chiba University, Chiba 263-8522, Japan

² Molecular Chirality Research Center, Chiba University, Chiba 263-8522, Japan

In organic semiconductors, the carrier transport occurs through the overlap of molecular orbitals. The intermolecular orbital interaction results in the split of energy levels. For the highest occupied molecular orbital (HOMO), the split of lead phthalocyanine (PbPc) dimer has been observed by ultraviolet photoelectron spectroscopy (UPS) [1]. Similar splitting can be observed for lowest unoccupied molecular orbital (LUMO) using low-energy inverse photoelectron spectroscopy (LEIPS) [2].

Recently, we demonstrated that tin-phthalocyanine (SnPc) film grows layer by layer into a quasi-1D columnar structure on graphite. From the low energy electron diffraction and UV-visible absorption measurements, we concluded that the structure is similar to the monoclinic phase of PbPc crystal [3]. We applied UPS and LEIPS to the SnPc films with the thickness between 2 and 5 monolayers (MLs). The observed characteristic broadening of peaks were interpreted as the energy level splits due to the intermolecular electronic coupling [4]. The initial aim of this study was to observe an energy-momentum dispersion relation of splitted HOMO peaks of SnPc bilayer using energy-dependent UPS. In the momentum space, the intensities of the two components are expected to vary [5] which should be decisive evidence of our interpretation.

In the experiment, a highly oriented pyrolytic graphite (HOPG) was cleaved in air and annealed at 873 K for 2 hours in vacuum. The 2 ML thick SnPc film was prepared by the vacuum deposition onto the HOPG at room temperature (300 K) for the UPS study.

Figure 1 shows energy-dependent UPS spectra. We observed a peak at 1.5 eV and a shoulder at 1.3 eV at the photon energy $h\nu$ of 40 eV at 25 min after the film preparation. The line shape is similar to our previous UPS results [4] suggesting that the spectral features originate from the split of SnPc dimer interaction. Subsequently, we measured the spectra at different photon energies, $h\nu = 105, 85$ and 70 eV. The line shapes became a single broad peak without shoulder. Finally, we measured again the spectrum at $h\nu=40$ eV 205 min after the sample preparation. The observed spectrum is completely different from the previous one as shown in Fig. 1.

The SnPc film shows polymorphs. When SnPc is deposited at the room temperature, the 1D columnar structure is observed. However, a different film having a head-to-tail molecular arrangement is observed when the film is prepared on a substrate at elevated

temperature or the film is annealed after the deposition [4]. This indicates that the 1D columnar structure is a metastable and transformed to the more stable head-to-tail arrangement. The relation of the two phases is similar to the monoclinic [3] and triclinic [6] phases of PbPc.

The observed difference in the spectral line shapes in this work is most likely due to the phase transition of Sn bilayer though the reason is not clear at the moment. Our previous UPS measurement was made at 290 K which is 10 K lower than the temperature of the present work at BL2B. This subtle difference may cause the phase transition. Also the contamination on the HOPG surface may affect the stability of the 1D-columnar phase.

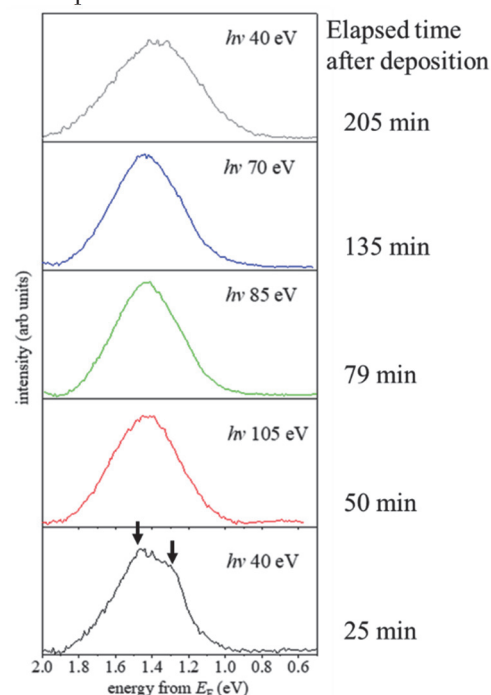


Fig. 1. Energy-dependent UPS spectra of 2 ML SnPc film on HOPG. Spectral features changed by elapsed time after deposition.

- [1] S. Kera *et al.*, Phys. Rev. B **75** (2007) 121305.
- [2] H. Yoshida, Chem. Phys. Lett. **539–540** (2012) 180.
- [3] Ukei, Acta Cryst. B **29** (1973) 2292.
- [4] Y. Kashimoto *et al.*, (submitted).
- [5] Moser, J. Electron Spectrosc. Relat. Phenom. **214** (2017) 29.
- [6] Iyechika *et al.*, Acta Cryst. B **38** (1982) 766.

BL2B

Internal Electric Potential Distributions in Metallo-phthalocyanine Thin Films: Magnesium Phthalocyanine and Aluminum Phthalocyanine Chloride

Y. Nakayama

Department of Pure and Applied Chemistry, Tokyo University of Science, Noda 278-8510, Japan

Phthalocyanines have been used as hole transporting materials in various prototypical organic semiconductor devices such as organic solar cells [1]. A striking point of metallo-phthalocyanines is the tunability of their electronic properties, e.g., energy gap width (color), molecular shape, and permanent dipole moment, by switching the metal species at the center of the ligand ring. In the present work, we conducted photoelectron spectroscopy (PES) measurements on thin films of two kinds of metallo-phthalocyanine molecules (Fig. 1), magnesium phthalocyanine (MgPc) and aluminum phthalocyanine chloride (AlClPc), to study electronic states of these materials.

MgPc and AlClPc thin film were deposited in a step-by-step manner under ultra-high vacuum (base pressure below 2×10^{-7} Pa) conditions onto Au-coated Si substrates. It should be noted that the Au/Si substrates had been prepared in a separate system and transferred in the ambient atmosphere, so that the surface of these was not clean but contained some contaminants. PES measurements were conducted at BL2B of UVSOR, IMS. The excitation photon energy was fixed at 120 eV throughout this work. In order to avoid any unfavorable shift or broadening of the spectra due to sample charging or radiation damage, measurement duration of each spectrum was minimized and also the photon flux was reduced to restrict the photoemission current not to exceed 100 pA. All the measurement were carried out in the normal emission geometry and at room temperature.

As shown in Fig. 2, the vacuum level and Mg2p states shifted to the lower energy side in increasing the MgPc thickness suggesting a downward band bending in the MgPc film toward the surface. The similar trend was previously reported for CuPc [2, 3]. In contrast, AlClPc exhibited substantially no (or slightly upward [4]) band bending in its thin film. As a result of this existence/absence of the band bending, the hole transporting state of MgPc shifted closer to the Fermi level as approaching the substrate (Fig. 3(a)), which is advantageous for extraction of holes to the Au electrode, whereas that of AlClPc are almost constant regardless of the film thickness (Fig. 3(b)).

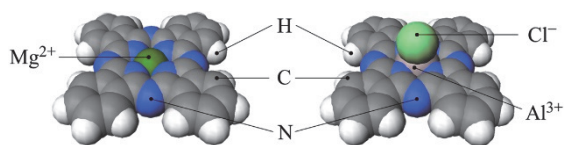


Fig. 1. Structures of MgPc (left) and AlClPc (right).

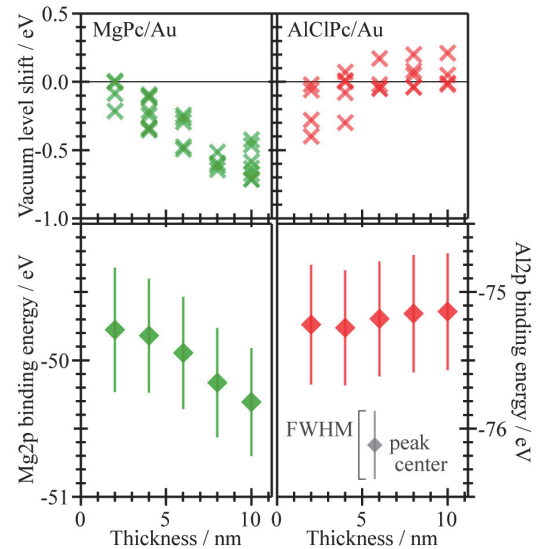


Fig. 2. Vacuum level shifts (upper panels) and core level peak positions (lower panels) of MgPc (left panels) and AlClPc (right panels) thin films on Au substrates plotted as a function of the film thickness.

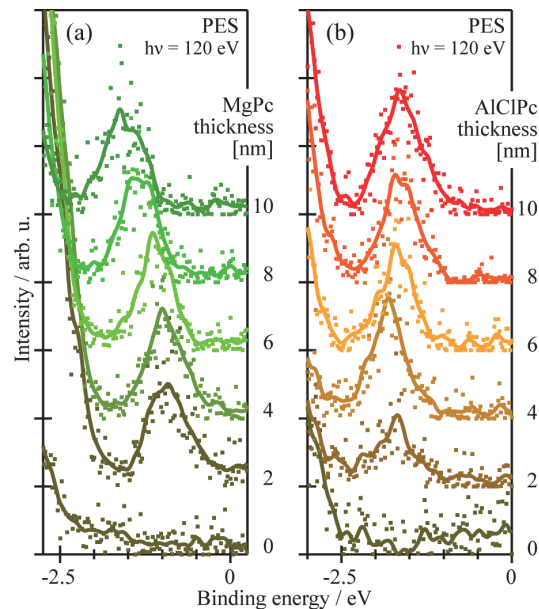


Fig. 3. Evolution of the PES spectra of the (a) MgPc and (b) AlClPc thin films.

- [1] C. W. Tang, *Appl. Phys. Lett.* **48** (1986) 183.
- [2] H. Yamane *et al.*, *J. Appl. Phys.* **99** (2006) 093705.
- [3] Y. Nakayama *et al.*, *Adv. Energy Mater.* **4** (2014) 1301354.
- [4] M.-K. Lin *et al.*, *Phys. Rev. B* **95** (2017) 085425.

BL2B

Effects of Water Exposure on Materials for Organic Light Emitting Diodes

Y. Nakayama, F. Minagawa and M. Hikasa

Department of Pure and Applied Chemistry, Tokyo University of Science, Noda 278-8510, Japan

Deterioration of organic semiconductor materials is a common drawback for organic electronic devices. Humidity is widely believed as a major factor that degrades functionalities of the materials, yet accurate mechanisms how water molecules impact the electronic states of the organic semiconductor materials are still not well understood. In the present works, effects of exposure to H₂O on representative organic materials for light emitting diodes (Fig. 1), 2,2',7,7'-tetrakis(*N,N*-di-*p*-methoxyphenylamino)-9,9'-spirobifluorene (spiro-OMeTAD) as a hole transporter [1], tris(8-hydroxyquinolino)aluminium (Alq₃) as an electron transporter and emitter [2], and dipyrazino[2,3-*f*:2',3'-*h*]quinoxaline-2,3,6,7,10,11-hexacarbonitrile (HATCN) as a hole injector [3], are studied by photoelectron spectroscopy (PES).

10 nm-thick spiro-OMeTAD, Alq₃, and HATCN were deposited onto Au/Si substrate in ultra-high vacuum conditions. Each sample was subsequently exposed to H₂O up to the dosage of 10⁸ L (1 L = 1 × 10⁻⁶ Torr·s) in a step-by-step manner. PES measurements were conducted at BL2B of UVSOR.

Figure 2 shows variation in the work function values of these three materials plotted as a function of dosage of H₂O. It was revealed that spiro-OMeTAD exhibits reduction of the work function by exposure to H₂O, whereas the work function of the Alq₃ thin film was preserved at the pristine value even after a 10⁸ L dosage of H₂O. For the HATCN case, the work function exhibited irregular jumps, which may be ascribed to position by position inhomogeneity of the HATCN film. However, the similar trend to the case of spiro-OMeTAD can be recognized, which supports reduction of the work function of HATCN due to exposure to the ambient atmosphere.

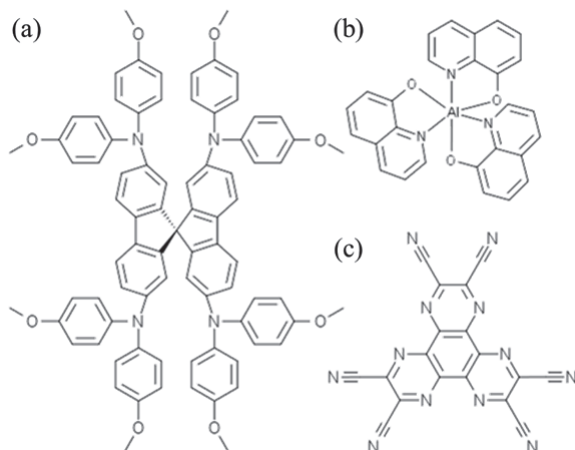


Fig. 1. Molecular structures of (a) spiro-OMeTAD, (b) Alq₃, and (c) HATCN.

PES spectra in the highest occupied molecular orbital (HOMO) regions of the spiro-OMeTAD and Alq₃ films evolved upon exposure to H₂O as shown in Fig. 3, in which each spectrum is plotted with respect to the vacuum level. The HOMO positions in these spectra are substantially maintained independent of the H₂O dosage, namely the water vapor in this dosage range does not rise any significant effects to the ionization energies of spiro-OMeTAD and Alq₃. The Fermi level (E_F) separated away from the HOMO of spiro-OMeTAD in increasing the dosage of H₂O, which may result in a disadvantage for the efficiency for hole injection into this material from electrodes.

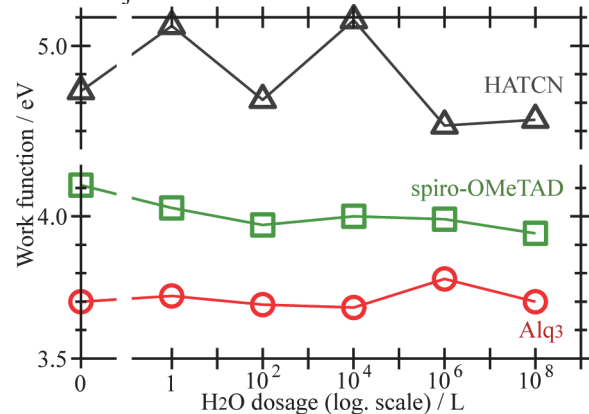


Fig. 2. Work function variation on exposure to H₂O.

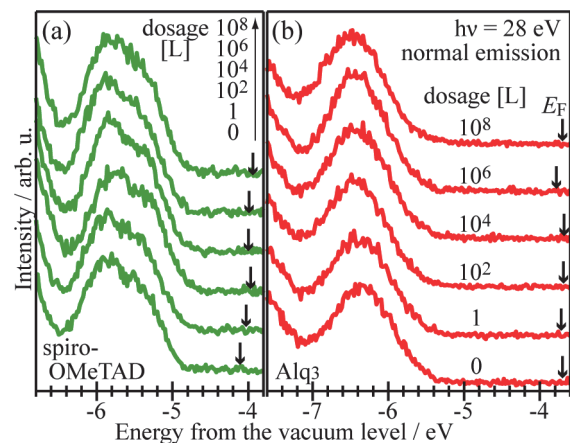


Fig. 3. Evolution of the PES spectra of 10 nm-thick (a) spiro-OMeTAD and (b) Alq₃ thin films upon exposure to H₂O. The E_F positions are indicated by downward arrows on the respective spectra.

[1] O. A. Jaramillo-Quintero *et al.*, *J. Phys. Chem. Lett.* **6** (2015) 1883.

[2] C. W. Tang *et al.*, *Appl. Phys. Lett.* **51** (1987) 913.

[3] S. Park *et al.*, *Appl. Phys. Lett.* **97** (2010) 063308.

BL3U

Cobalt Oxide Catalyst Containing Glycine Molecule Studied by Operando O K-edge XAFS Measurement

M. Yoshida^{1,2,*}, T. Hiue³, M. Nagasaka⁴, H. Yuzawa⁴, N. Kosugi⁴ and H. Kondoh³

¹Yamaguchi University, Yamaguchi, 755-8611, Japan

²Cooperative Research Fellow, Institute for Catalysis, Hokkaido University, Sapporo 001-0021, Japan

³Keio University, Yokohama 223-8522, Japan

⁴Institute for Molecular Science, Okazaki 444-8585, Japan

Electrochemical water splitting using renewable energies such as solar, wind, and hydroelectric powers is one of the promising methods for sustainable hydrogen production. In this system, oxygen evolution reaction (OER) limits the efficiency of overall water splitting due to the high overpotential. Thus, the development of highly active OER electrocatalyst is strongly required. Recently, Nocera and co-workers reported cobalt-phosphate-based catalyst (Co-P_i) could function as the efficient OER catalyst [1]. On the other hand, our group found that nickel oxide clusters were integrated by amino acids and the catalytic activity was enhanced [2]. Herein, we examined whether the OER activity was improved by addition of organic molecules to Co-P_i, and the function of the organic molecule was investigated using operando UV-vis absorption, X-ray absorption fine structure (XAFS), and infrared absorption spectroscopy in an attenuated total reflection mode (ATR-IR).

A Teflon electrochemical cell was equipped with a Pt wire counter electrode and a Ag/AgCl reference electrode for all electrochemical experiments. Cobalt oxide thin films were electrodeposited on an indium tin oxide (ITO), a Pt/Pd thin film, or a Au thin film in potassium phosphate (K-P_i) containing Co(NO₃)₂ and glycine (Co-Gly). The prepared sample was investigated using operando UV-vis absorption, XAFS, and ATR-IR.

Constant potential electrolysis was conducted in a potassium phosphate (K-P_i) aqueous electrolyte. The OER current of Co-Gly was higher than that of Co-P_i, indicating that the glycine molecule enhanced the OER activity of Co-P_i. To assess the film thickness of these catalysts, the operando UV-vis absorption spectra were taken and we found that the glycine molecule promoted the electrodeposition of cobalt oxide catalyst. Next, to investigate the local structure of Co species in the Co-Gly, Co K-edge extended X-ray absorption fine structure (EXAFS) spectra were taken for Co-Gly and CoOOH reference powder. This result suggested that the local structure of Co species in the Co-Gly was composed of an edge-sharing CoOOH octahedral clusters a few nanometers in size. Moreover, to observe the glycine species in Co-Gly, ATR-IR spectra were obtained and two upward bands attributed to the adsorbed glycine species was observed during the electrodeposition of Co-Gly

catalysts.

Finally, operando O K-edge XAFS spectra for Co-Gly were taken under electrochemical control with transmission mode at BL3U in the UVSOR Synchrotron, according to the previous works [3]. An absorption peak assigned to CoOOH was observed around 530 eV. Meanwhile, when the electrode potential was changed from 0.5 V to 1.0 V, a peak attributed to the CoO₂ species was observed around 529 eV as the active species for OER process.

In conclusion, we found that the glycine molecule combined between cobalt oxide clusters composed of CoOOH octahedral structure and the OER activity was enhanced because the number of active reaction sites (CoO₂) increased.

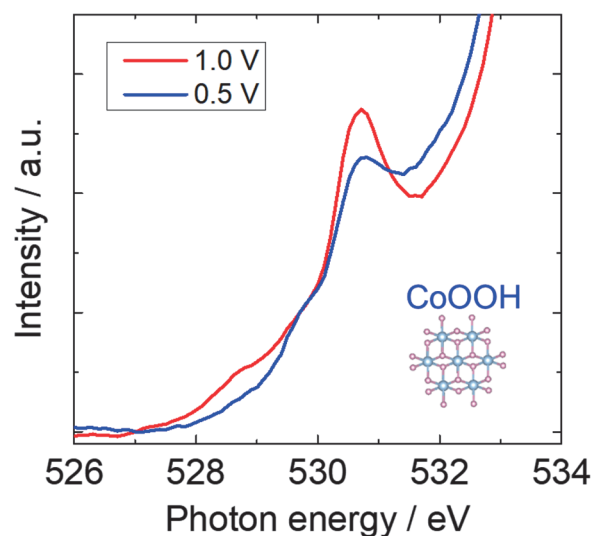


Fig. 1. Operando O K-edge XAFS spectra for Co-Gly catalyst.

[1] D. G. Nocera *et al.*, *Science* **321** (2008) 1072.

[2] M. Yoshida* *et al.*, *J. Phys. Chem. C* **121** (2017) 255.

[3] (a) M. Nagasaka *et al.*, *J. Phys. Chem. C* **117** (2013) 16343. (b) M. Yoshida* *et al.*, *J. Phys. Chem. C* **119** (2015) 19279.

BL3B

Effects of UV Irradiation and Annealing on the Oxygen Vacancies in Solution-processed IGZO Thin Films

 Y. Takamori^{1,3}, T. Morimoto^{1,3}, N. Fukuda³ and Y. Ohki^{1,2}
¹Waseda University, Tokyo 169-8555, Japan

²Research Institute for Materials Science and Technology, Waseda University, Tokyo 169-8555, Japan

³Flexible Electronics Research Center (FLEC), National Institute of Advanced Industrial Science and Technology (AIST), Tsukuba 305-8565, Japan

We fabricated solution-processed IGZO thin film transistors (TFTs) [1], and found that the drain current in the TFTs decreases by UV irradiation and recovers by thermal annealing. In this paper, the mechanism of this phenomenon was analyzed by photoluminescence (PL) and XPS measurement.

The IGZO precursor solution was prepared by dissolving nitrate hydrates of In, Ga and Zn with a molar ratio of 6:1:3 in a solvent consisting of 2-methoxyethanol and 2, 2, 2-trifluoroethanol with a volume ratio of 4:1. This solution was spin-coated on a 300-nm thick thermally oxidized SiO₂ fabricated on a p-type Si substrate, and sintered at 250 °C on a hot plate in air for 1 h. Then, Al electrodes were vacuum-evaporated onto the IGZO film to fabricate a bottom-gate top-contact TFT with a channel length of 50 μm and a channel width of 500 μm.

Figure 1 shows transfer characteristics of the IGZO TFTs at drain voltage $V_D = 40$ V. Their drain currents decrease by 7.21 eV UV irradiation from a Xe₂* excimer lamp (UER20-172, Ushio) and recover by the subsequent thermal annealing at 250 °C on a hot plate in air for 30 min.

Figure 2 shows broad PL spectra of the IGZO films, excited by 4.6-eV photons at 10 K. The intensity of this PL peak centered at nearly 2.25 eV increases by the UV irradiation and decreases by the subsequent thermal annealing. This PL originates from oxygen vacancies [2]. Next, XPS O 1s peaks observed in the IGZO films were separated into three components by Gaussian fitting. The lowest component O_I at 530.2 eV is due to lattice oxygens. The middle component O_{II} at 531.7 eV is due to oxygens in oxygen-deficient regions. The highest component O_{III} at 532.7 eV is due to loosely bound oxygens on the surface of the films, such as -CO₃, adsorbed H₂O, or adsorbed O₂ [3]. Figure 3 shows the intensity ratio of each component. The O_{II} increases by the UV irradiation and decreases by the subsequent thermal annealing.

We have reported that oxygen vacancies can act as electron scattering centers and that the increase of oxygen vacancies occurs as the Ga content in solution-processed IGZO films increases. Namely, oxygen vacancies decrease the drain current [2]. These results indicate that the decrease in drain current induced by the UV irradiation is also due to the increase in number of oxygen vacancies.

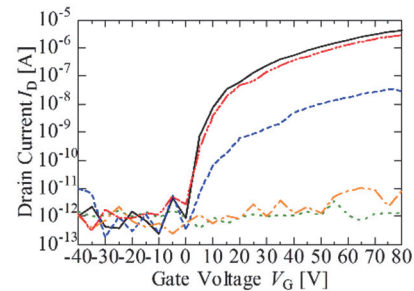


Fig. 1. Transfer characteristics of the IGZO TFTs at $V_D = 40$ V before the UV irradiation (—), after the UV irradiation for 1 (---), 5 (···), and 10 min (-·-), and after the subsequent thermal annealing (-·-).

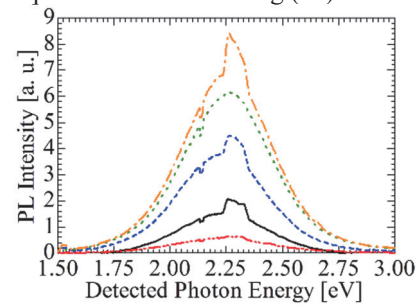


Fig. 2. PL spectra of the IGZO thin films, excited by 4.6-eV photons at 10 K before the UV irradiation (—), after the UV irradiation for 1 (---), 5 (···), and 10 min (-·-), and after the subsequent thermal annealing (-·-).

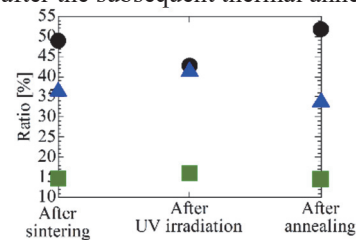


Fig. 3. Intensity ratios of the three components of XPS O 1s peaks: O_I due to lattice oxygens (●), O_{II} due to oxygens in oxygen-deficient regions (▲), and O_{III} due to loosely bound oxygens on the surface of the IGZO films (■), before and after the UV irradiation for 10 min, and after the subsequent thermal annealing.

[1] S. Ogura *et al.*, *Flex. Print. Electron.* **1** (2016) 045001.

[2] Y. Ochiai *et al.*, *UVSOR Activity Report* **44** (2017) 128.

[3] G. H. Kim *et al.*, *Thin Solid Films*, **517** (2009) 4007.

BL4B

Substrate-symmetry Driven Electronic and Magnetic Modifications in a Monatomic Layer Iron Nitride

T. Miyamachi¹, T. Hattori¹, S. Nakashima¹, Y. Takagi^{2,3}, T. Yokoyama^{2,3} and F. Komori¹

¹*Institute for Solid State Physics, University of Tokyo, Kashiwa 277-8581, Japan*

²*Department of Materials Molecular Science, Institute for Molecular Science, Okazaki 444-8585, Japan*

³*Department of Structural Molecular Science, The Graduate University for Advanced Studies (SOKENDAI), Okazaki 444-8585, Japan*

Iron nitrides have a variety of compositions and crystal structures depending on the nitrogen concentration. Especially, the iron rich Fe₄N phase attracts great attention toward practical application for its high coercivity and room temperature ferromagnetism in the form of thin films [1]. Fe₄N thin films can be grown on Cu(001) with alternating Fe- and Fe₂N- planes in the fcc Fe sublattice with a N atom centered in the cubic cell. At the thinnest limit, i.e., a monatomic layer, the Fe₂N plane preferentially grows on the surface and the surface reconstruction from the square c(2×2) lattice in bulk to the p4gm(2×2) one takes place, which is so called clock reconstruction [1, 2].

Using scanning tunneling microscopy (STM) and low energy electron diffraction (LEED), we have recently revealed the high stability of the p4gm(2×2) lattice in the monatomic layer Fe₄N (Fe₂N) due to the strong bonding between Fe and N atoms [3,4]. Furthermore, with the help of x-ray absorption spectroscopy/x-ray magnetic circular dichroism (XAS/XMCD) and the first principles calculations, the strong in-plane magnetic anisotropy observed for the Fe₂N is successfully associated with the change in the distribution of Fe 3d electrons by the electronic hybridization with Cu (001) [5]. In this work, taking the advantage of the robust surface lattice of the Fe₂N, we intend to tune its magnetic properties by changing the supporting substrate symmetry from fourfold Cu(001) to threefold Cu(111). This can modify the degrees of the binding and thus of the electronic hybridization between the Fe₂N and the substrate.

The growth and structural properties of the Fe₂N on Cu(111) were pre-checked by STM before XAS/XMCD [6]. Likewise on Cu(001) [3-5], N⁺ ions with an energy of 500 eV were firstly bombarded to the clean Cu(111) surface and Fe was additionally deposited at room temperature. By subsequent annealing at 620 K, well-ordered Fe₂N was grown on the surface. We find that the Fe₂N keeps the clock reconstruction even on Cu(111), while the moiré pattern additionally appears on the surface due to the slight lattice distortion of the Fe₂N. Note that the

sample quality for XAS/XMCD is confirmed from the consistency of Fe₂N LEED patterns in STM and XAS/XMCD measurements.

The measurements were performed at BL4B in UVSOR by total electron yield mode at B = ± 5 T and T = 6.2 K. The XMCD spectra are obtained at the normal (NI: θ = 0°) and the grazing (GI: θ = 55°) geometries by detecting μ₊ - μ₋, where μ₊ (μ₋) denotes the XAS recorded at Fe L-adsorption edges with the photon helicity parallel (antiparallel) to the sample magnetization. Note that θ is the angle between the sample normal and the incident x-ray.

We find that the XMCD intensity is slightly greater in the GI geometry than in the NI geometry. This reveals that the magnetic easy axis of the Fe₂N on Cu(111) is towards in-plane direction as in the case on Cu(001). However, the spin magnetic moment of the Fe₂N on Cu(111) is quantitatively evaluated to be ~ 0.5 μ_B/atom from XMCD sum rules, which is considerably smaller than that on Cu(001) of ~ 1.1 μ_B/atom [5]. Furthermore, the magnetization curves of the Fe₂N on Cu(111) recorded in the NI and GI geometries behave in a similar fashion, while the strong in-plane magnetic anisotropy is confirmed for the geometry dependence of the magnetization curve on Cu(001) [5]. The results indicate that changing the symmetry of the supporting substrate from Cu(001) to Cu(111) modifies electronic properties of the Fe₂N especially for Fe 3d states, and accordingly magnetically weakens the Fe₂N.

In future work, combining results of XMCD with those of STM and the first principles calculations, we will discuss the impacts of the atomic-scale distortion and surface inhomogeneity including moiré corrugation on the electronic and magnetic properties of the Fe₂N on Cu(111).

[1] J. M. Gallego *et al.*, Phys. Rev. B **70** (2004) 115417.

[2] Y. Takagi *et al.*, Phys. Rev. B **81** (2010) 035422.

[3] Y. Takahashi *et al.*, Phys. Rev. Lett. **116** (2016) 056802.

[4] K. Ienaga *et al.*, Phys. Rev. B **96** (2017) 085439.

[5] Y. Takahashi *et al.*, Phys. Rev. B **95** (2017) 224417.

[6] T. Hattori *et al.*, Phys. Rev. M *accepted*.

BL4B

Interfacial Spin and Orbital Magnetic Moments and their Anisotropies in Pd Studied by X-ray Magnetic Circular Dichroism in Co/Pd Multilayers

J. Okabayashi^{1,*}, Y. Miura² and H. Munekata³¹Research Center for Spectrochemistry, The University of Tokyo, Tokyo 113-0033, Japan²Electrical Engineering and Electronics, Kyoto Institute of Technology, Kyoto 606-8585, Japan³Laboratory for Future Interdisciplinary Research Science and Technology, Tokyo Institute of Technology, Yokohama 226-8503, Japan

Ultrathin Co/Pd multilayers are artificial nanomaterials that exhibit perpendicular magnetic anisotropy (PMA), due to the spin-orbit interactions, achieved through interfacial chemical bonding. Extensive efforts have been made for studying interfaces of ultra-thin magnetic multilayers and nanostructures. Studies on Co atoms performed using X-ray magnetic circular dichroism (XMCD) have suggested the enhancement of orbital magnetic moments at the interfacial Co that is adjacent to Pd. It has been reported that the PMA emerges due to the cooperative effects between spin moments in *3d* TMs and large spin-orbit interactions in the non-magnetic *4d* or *5d* TMs. However, the interfacial PMA, including the anisotropic orbital magnetic moments, has not been fully understood for both Co and Pd sites. Bruno and van der Laan theoretically proposed an orbital moment anisotropy in *3d* TMs within the second-order perturbation of the spin-orbit interaction for more than half-occupied electrons [1]. However, in the case of strong spin-orbit coupling in *4d* or *5d* TMs, the validity of this perturbative formula has been debated [2]. In order to study the mechanisms of PMA in Co/Pd multilayers, the orbital magnetic moments contributions of each element have to be explicitly considered. It is challenging to study the anisotropy of the orbital magnetic moments of both Co and Pd elements using one specific experiment, due to the challenges in detection of the induced magnetic moments, of Pd in particular.

For the interfacial Pd, the magnetic dipole contribution through the quadrupole interactions between dipoles is assessed quantitatively. We focus on the anisotropy of orbital moments at the Co/Pd interfaces using XMCD and first-principles density functional theory (DFT) calculations, which provide the element- and layer-resolved contributions that reveal the mechanism of PMA.

We prepared the sample of Co/Pd multilayered structures: Co (0.69 nm)/Pd (1.62 nm) for PMA with stacking five periods on the Si substrates [3]. Sample surfaces were sputtered by Ar ions before the XMCD measurements in order to remove the oxygen contamination. We performed XMCD experiments at BL4B, UVSOR, Institute of Molecular Science. Total electron yield mode by directly detecting the sample current was adopted. A magnetic field of ± 5 T was applied along the direction of the incident polarized soft x-ray.

We successfully observed clear XMCD signals in Pd

M-edges after the removal of surface contamination as shown in Fig. 1. Although the XAS line shapes overlap with those of O *K*-edge absorption, clear XMCD signals induced by the proximity with Co layers are observed. The Pd *M*-edge XMCD line shapes are almost identical, which suggests isotropic orbital moments in Pd, within the detection limits. This indicates that the isotropic finite orbital moments in Pd do not directly contribute to the PMA. On the other hand, clear Co *L*-edge XAS and XMCD with angular dependence reveal the enhancement of orbital moments in the surface normal direction because of PMA.

Next, we discuss the quadrupole-like contribution of the interfacial Pd layer. Our Pd XMCD results indicate that the Pd orbital moments induced at the interface are isotropic. Note that the magnetic dipole term m_T is an order of magnitude smaller than the orbital moments, i.e., less than $0.005 \mu_B$, comparable with the detectable limits. Therefore, the relatively large spin-orbit coupling constant and small Pd exchange splitting contribute to the appearance of PMA by means of quadrupole-like interactions through the interfacial proximity effects. Furthermore, these results are well explained by DFT calculations.

We acknowledge to Prof. T. Yokoyama, Dr. Y. Takagi, and Dr. K. Uemura for the technical supports at BL4B.

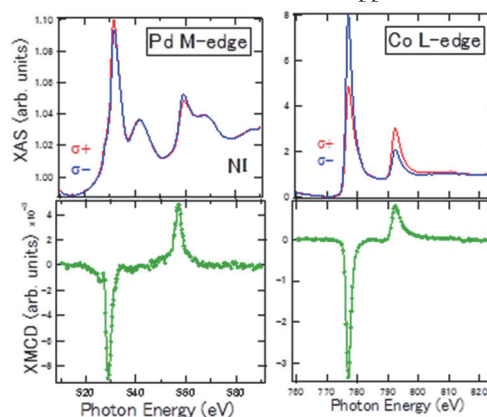


Fig. 1. XAS and XMCD of Pd *M*-edge and Co *L*-edge in perpendicularly magnetized Co/Pd multilayer.

- [1] P. Bruno, Phys. Rev. B **39** (1989) 865.
- [2] C. Andersson *et al.*, Phys. Rev. Lett. **99** (2007) 177207.
- [3] K. Yamamoto *et al.*, IEEE TRANSACTIONS ON MAGNETICS **49** (2013) 3155.

*e-mail: jun@chem.s.u-tokyo.ac.jp

BL4B

Magnetic Properties of Magnetic Ionic Liquid Thin Films Prepared on Cu(001) and Ferromagnetic Co/Cu(001)

K. Eguchi¹, T. Yokoyama^{2,3} and K. Awaga¹¹Department of Chemistry, Nagoya University, Nagoya 464-8602, Japan²Department of Materials Molecular Science, Institute for Molecular Science, Okazaki 444-8585, Japan³School of Physical Sciences, The Graduate University for Advanced Studies (SOKENDAI), Okazaki 444-8585, Japan

Ionic liquids (ILs), which consist of mobile cations and anions at near-room temperature, have attracted much attention in a wide range of applications because of their unique properties such as low melting points, non-volatility, and high capacitance. ILs are generally non-magnetic; however, incorporating magnetic ions into ILs at room temperature yields paramagnetic ILs [1, 2]. Magnetic susceptibility measurements have been performed to understand the magnetic properties of magnetic ILs [1, 2]. However, to the best of our knowledge, their magnetic properties on metal substrates have not been reported. This study investigates the magnetic properties of 1-ethyl-3-methylimidazolium tetrachloroferrate ([Emim][FeCl₄], Fig. 1(a)) thin films prepared on Cu(001) using X-ray magnetic circular dichroism (XMCD) measurements. These measurements were also performed for [Emim][FeCl₄] thin films prepared on ferromagnetic Co/Cu(001) to examine the magnetic interaction between trivalent Fe ions in FeCl₄⁻ and Co thin films at the interfaces.

A commercially available [Emim][FeCl₄] (Tokyo Chemical Industry) was deposited on Cu(001) and Co(3 ML)/Cu(001) [3] at room temperature using a pulse valve under ultrahigh vacuum ($P \sim 10^{-7}$ Pa) conditions. The thickness of [Emim][FeCl₄] was set as 0.8 ML by controlling the opening time of the pulse valve. X-ray absorption spectroscopy (XAS) and XMCD measurements were performed using an XMCD system ($P < 1 \times 10^{-8}$ Pa, $B = 7$ T, and $T = 3.8$ K). XMCD spectra were obtained by the total electron yield detection mode in a magnetic field of ± 5 mT or ± 5 T at a temperature of 6.5 K and an X-ray incidence angle of 55° with respect to the surface normal.

The [Emim][FeCl₄] thin film prepared on Cu(001) showed an XMCD signal at the Fe *L*-edge in a magnetic field of 5 T (Fig. 1(b)). The effective spin (m_{spin}) and orbital (m_{orb}) magnetic moments of the trivalent Fe ion in the thin film were calculated using the sum rules [4,5], wherein $m_{\text{spin}} = 1.82 \mu_B$ and $m_{\text{orb}} = 0.15 \mu_B$; here, the number of *d*-holes was assumed as 5. Considering the Brillouin function at $T = 6.5$ K and $B = 5$ T, the value of m_{spin} is almost identical to the magnetic moment of $2.03 \mu_B$ for $S = 3/2$. The magnetic property of the [Emim][FeCl₄] thin film prepared on Co/Cu(001) was similar compared with that prepared on Cu(001), indicating weak magnetic interactions of Fe with Co at $T = 6.5$ K (Figs. 1(c) and 1(d)).

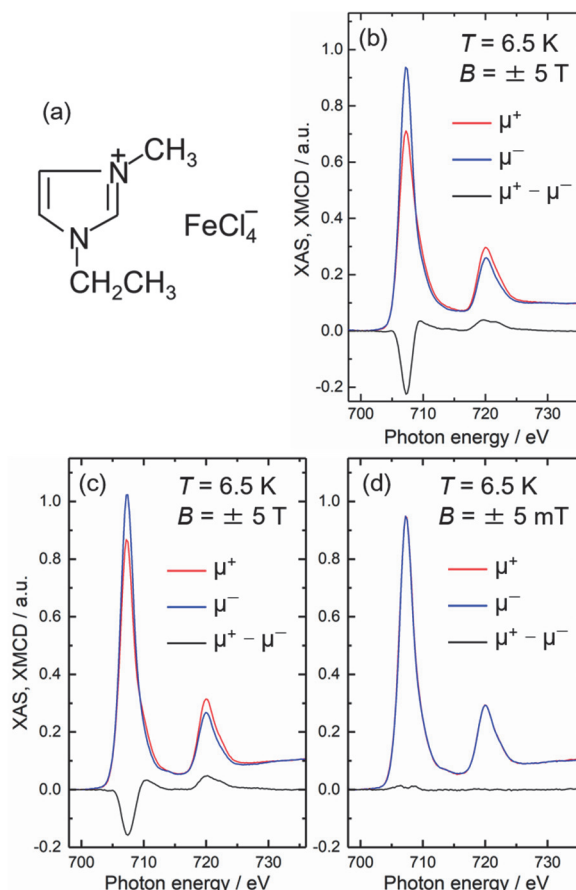


Fig. 1. (a) Chemical structure of [Emim][FeCl₄]. Fe *L*-edge X-ray absorption and X-ray magnetic circular dichroism spectra of [Emim][FeCl₄] on (b) Cu(001) and (c,d) Co (3 ML)/Cu(001).

[1] S. Hayashi and H. Hamaguchi, Chem. Lett. **33** (2004) 1590.

[2] Y. Yoshida, *et al.*, Bull. Chem. Soc. Jpn. **78** (2005) 1921.

[3] K. Eguchi, *et al.*, J. Phys. Chem. C **118** (2014) 17633.

[4] B.T. Thole, *et al.*, Phys. Rev. Lett. **68** (1992) 1943.

[5] P. Carra, *et al.*, Phys. Rev. Lett. **70** (1993) 694.

BL4B

XMCD Measurements on a Magnetic Topological Heterostructure: Mn and Te Deposited Bi_2Te_3

S. Kusaka¹, K. Yokoyama¹, Y. Uemura², T. Yokoyama² and T. Hirahara¹¹Department of Physics, Tokyo Institute of Technology, Tokyo 152-8551, Japan²Department of Materials Molecular Science, Institute for Molecular Science, Okazaki 444-8585, Japan

Topological insulators (TI) are extensively studied recently due to its peculiar properties [1]. The Dirac-cone surface states of TI are protected by time-reversal symmetry (TRS) and backscattering among these surface states is prohibited. But when TRS is broken by application of a magnetic field or incorporating magnetic materials, a gap opening in the Dirac cone is expected and an intriguing phase called the quantum anomalous Hall state can be realized [2]. This phase is expected to show even more exotic phenomena such as the topological magnetoelectric effect. To realize such state, two types of sample fabrication techniques have been employed up to now: (1) magnetic doping while growing the single crystal or thin film of TI [3], and (2) magnetic impurity deposition on the surface of TI [4]. While method (1) was successful and showed evidence of the TRS violation, no one has succeeded using method (2), which should be a more direct way to examine the interaction between the topological surface states and magnetism. Recently, we have succeeded in inducing a gap in the TI Dirac surface states by a new method called ‘magnetic extension’ [5]. An ordered Mn layer was incorporated into the topmost quintuple layer of a prototypical TI, Bi_2Se_3 by Mn and Se deposition and a $\text{MnBi}_2\text{Se}_4/\text{Bi}_2\text{Se}_3$ heterostructure was formed. Due to the large wave function overlap between the Dirac cone and the ferromagnetic Mn layer, a large gap of 85 meV was observed and its origin was ambiguously assigned to the ferromagnetic nature of MnBi_2Se_4 as proven by XMCD measurements [6].

We have recently found that we can also employ magnetic extension to break the time reversal symmetry of another prototypical TI, Bi_2Te_3 . We deposited Mn and Te on Bi_2Te_3 and found a clear gap opening of ~ 70 meV at the Dirac point. In the present work, we have performed XMCD measurements at BL-4B to experimentally prove that this system is ferromagnetic. Figure 1 shows the X-ray absorption (XAS) spectra and the corresponding XMCD spectra at 5 T (~ 5 K). One can find clear XMCD peaks at the Mn L_3 and L_2 edges. The measurements were also performed at remanence, and the result is shown in Fig. 2. Although very weak, one can find a dip structure at the L_3 edge and this shows that this system is indeed ferromagnetic.

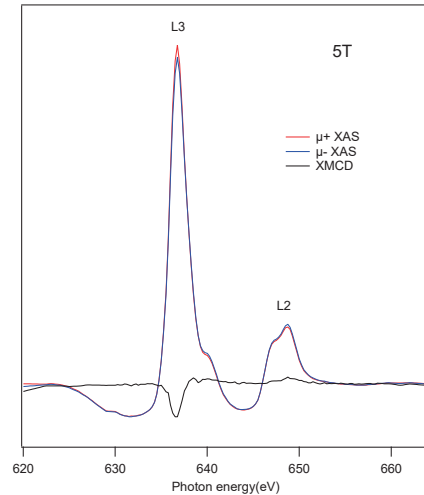


Fig. 1. XAS and XMCD spectra at 5 T.

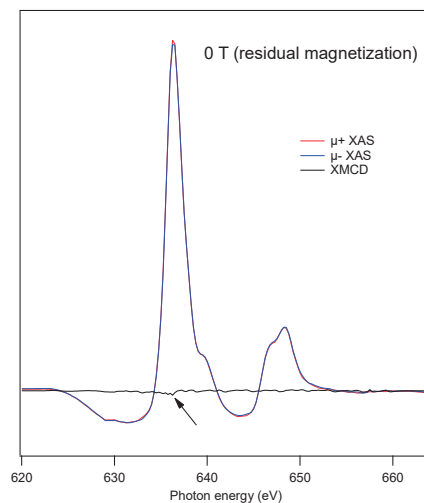


Fig. 2. XAS and XMCD spectra at 0 T (residual magnetization).

- [1] M. Hasan and C. Kane, *Reviews of Modern Physics* **82** (2010) 3045.
- [2] X.-L. Qi and S.-C. Zhang, *Reviews of Modern Physics* **83** (2011) 1057.
- [3] For example, C. Z. Chang *et al.*, *Science* **340** (2013) 167.
- [4] For example, M. Ye *et al.*, *Physical Review B* **85** (2012) 205317.
- [5] M. Otrokov *et al.*, *2D Mater.* **4** (2017) 025082.
- [6] T. Hirahara *et al.*, *Nano Letters* **17** (2017) 3493.

BL4B

Oxygen Induced Magnetic Transition in Single Layer Iron Film

T. Nakagawa¹, T. Nomitsu¹, S. Mizuno¹ and T. Yokoyama²

¹ Department of Molecular and Material Sciences, Kyushu University, Kasuga, Fukuoka 816-0955, Japan

² Institute for Molecular Science, Okazaki 444-8585, Japan

Molecular adsorption on magnetic thin films changes the magnetic anisotropy and the magnetization easy axis through the modification of the magnetic orbital moment, and thus induces a spin reorientation transition (SRT). It is not clear, however, whether molecular adsorption induces magnetic transitions, except the SRT, such as a ferromagnetic to antiferromagnetic transition since the exchange interaction is larger compared with the magnetic anisotropy energy.

Experiments were performed in the x-ray magnetic circular dichroism (XMCD) endstation with the base pressures of 4×10^{-8} Pa for sample preparation and better than 1×10^{-8} Pa for XMCD measurement. Single Fe layers were grown on W(110). Oxygen was dosed with the sample kept at the room temperature, via a variable leak valve at 2×10^{-7} Pa. The Fe films exposed up to 150 L (1 L = 1.3×10^{-4} Pa s) oxygen were examined by XMCD. The oxygen coverage was estimated by the appearance of an ordered 3×2 structure with 0.33 ML oxygen on Fe/W(110) using low energy electron diffraction [1]. Fe *L* edge XMCD was taken with a circularly polarized light (circularly polarization ~ 0.6) at $H = \pm 5$ T at a sample temperature of 6 K. NEXAFS spectra were measured at $H = 0$ T. All the measurements were performed for a grazing incidence angle of 30° from the surface.

Figure 1 (a) shows magnetization curves measured at Fe *L* edge. On the clean single layer Fe, the magnetization curve exhibits hysteresis and a large coercivity of ~ 2 T. With increasing the oxygen coverage, the magnetization and the coercivity decrease up to 0.33 ML oxygen coverage. At 0.33 ML, the Fe film is not ferromagnetic, and it is likely paramagnetic. The oxygen adsorption of 0.6 ML restores the Fe film to the ferromagnetic state with ~ 2 T coercivity. Further increase of the oxygen coverage, leading to the formation of iron oxide, transforms the Fe film to a non-ferromagnetic state.

In order to investigate the origin of the magnetic transition, we have measured NEXAFS spectra of O *K* edge with increasing the oxygen coverage. Figure 1(b) shows NEXAFS for the oxygen coverage of 0.33, 0.6 and 1 ML. For all the coverages studied the oxygen dissociates on the Fe film. At 0.33 ML, the peak at 530 eV is assigned to the transition to O(2p). The peak shifts to a higher energy with increasing the oxygen coverage. This energy shift is due to the strong hybridization between O 2p and Fe 3d, which would drive the transition from the paramagnetic to ferromagnetic state.

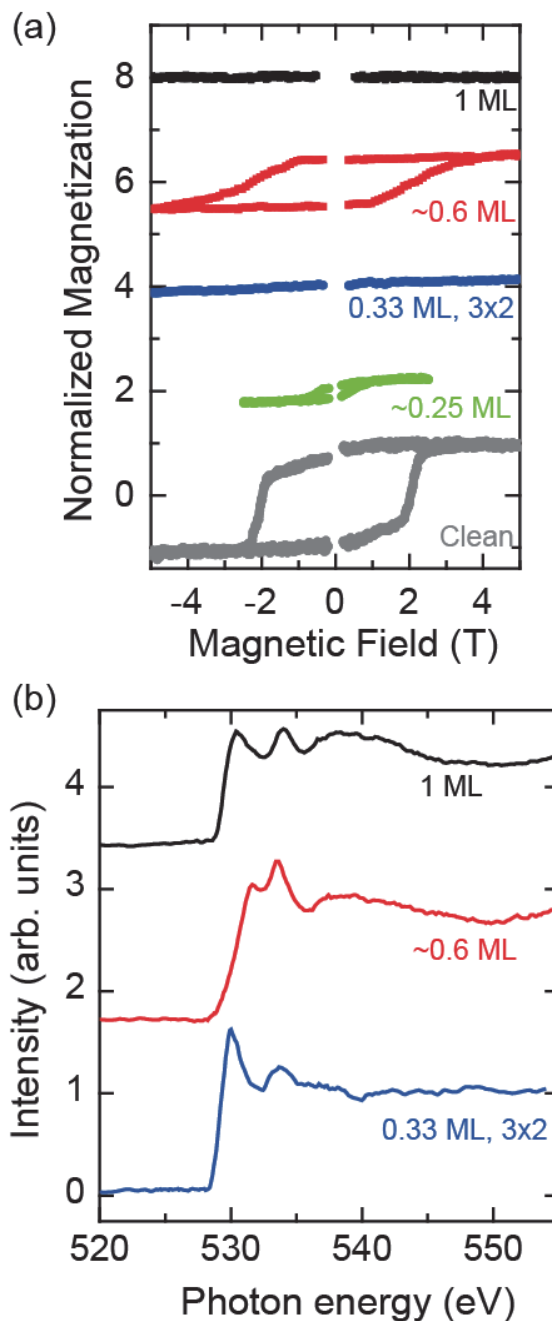


Fig. 1. (a) Magnetization curves measured at Fe-L edges. (b) NEXAFS for oxygen K edge. Indicated inside are the oxygen coverages.

[1] K. Feindl *et al.*, Surf. Sci. **617** (2013) 183.

BL5U

Change in the Electronic Structure of Fe₂P(10-10) Induced by Phosphorus Segregation: Soft X-ray Photoemission Spectroscopy Study

H. Motoyama¹, Y. Sugizaki¹, Y. Shimato¹, T. Yoshida¹, T. Takano¹ and K. Edamoto^{1,2}

¹Department of Chemistry, Rikkyo University, Tokyo 171-8501, Japan

²Research Center for Smart Molecules, Rikkyo University, Tokyo 171-8501, Japan

The surface properties of transition metal phosphides (TMPs) have attracted much attention because of their high catalytic performance for HDS and HDN for petroleum fuels. It has been found that Ni₂P has the highest catalytic activity among TMPs while that of Fe₂P is extremely low [1]. Therefore, in order to elucidate the origin of the high catalytic activity of TMPs, it is useful to explore the difference in the surface electronic structures of Ni₂P and Fe₂P. In this work, we investigated the phosphorus segregation process and its effect on the electronic structure of Fe₂P(10-10).

Our previous Auger electron spectroscopy (AES) study revealed that the P atoms on Fe₂P(10-10) are selectively removed by Ar⁺ ion sputtering. When the sputtered surface is subsequently annealed, the intensity ratio of P LMM and Fe MVV peaks in AES spectra decreases with elevating annealing temperature up to 400 °C, and increases at temperatures higher than 400 °C, as shown in the inset of Fig. 1. The P 2p spectrum of Fe₂P(10-10) after Ar⁺ ion sputtering, which was measured under a highly surface sensitive condition ($h\nu = 170$ eV), is shown in Fig. 1. The spectrum can be fit by seven components denoted as $\alpha - \eta$. The δ peak is assigned as a bulk component [2]. The analyses of annealing temperature dependence of the spectra show that the ϵ' , ζ , η peaks should be associated with weakly bonded surface species which would be formed through the sputtering, and α , β , γ , ϵ peaks are associated with surface P atoms segregated from the bulk. (The ϵ' and ϵ peaks are thought to be observed in the same binding energy region accidentally.) The former species are easily removed by annealing at lower than 400 °C, and the latter species are increased in intensities by annealing at higher than 300 °C, which are consistent with the AES results shown in the inset of Fig. 1.

Figure 2 shows the valence band spectra of Fe₂P(10-10) after Ar⁺ ion sputtering and subsequent annealing at various temperatures at 300 – 700 °C. The band observed at 0 – 4 eV is associated with the Fe 3d – P 3p hybrid band [2]. As shown in Fig. 2, the spectral shape of the band in the vicinity of E_F is not changed by the segregation of P atoms induced by heating above 400 °C, suggesting that the Fe 3d states are not stabilized by the bonding with segregated P atoms. This is contrary to the case of Ni₂P surfaces where the Ni 3d states are stabilized through the bonding with segregated P atoms forming a pseudo gap around E_F [3]. These results suggest that the stabilization of the

active metal sites through the bonding with P atom is crucial to maintain the activity during HDS through preventing the accumulation of S atoms on active metal sites.

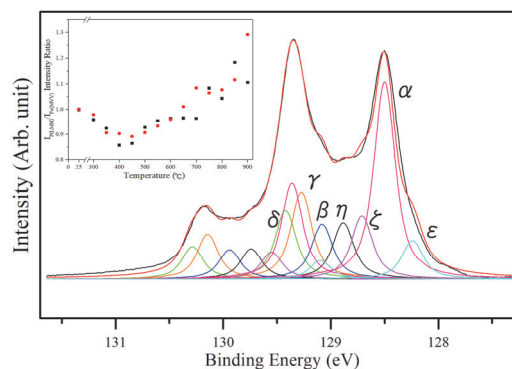


Fig. 1. The P 2p spectrum of Fe₂P(10-10) fit by Voigt functions. The change in the P LMM and Fe MVV Auger peak intensity ratio as a function of annealing temperature is shown in the inset.

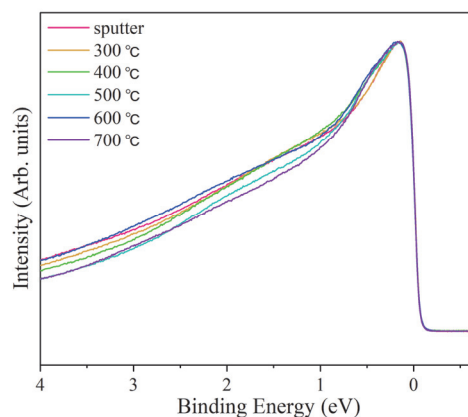


Fig. 2. Valence band spectra of Fe₂P(10-10) after Ar⁺ ion sputtering and subsequent annealing at various temperatures at 300 – 700 °C.

- [1] S. T. Oyama *et al.*, *Catal Today* **143** (2009) 94.
- [2] Y. Sugizaki *et al.*, *Surf. Sci.* **664** (2017) 50.
- [3] K. Edamoto, *Appl. Surf. Sci.* **269** (2013) 7.

BL5U

Valence-Band Electronic Structures of Ultra-Thin Fe Layers on Rashba-Split Au (111) Surfaces

J. Okabayashi^{1*}, K. Tanaka² and S. Mitani³

¹Research Center for Spectrochemistry, The University of Tokyo, Tokyo 113-0033, Japan

²UVSOR Synchrotron Facility, Institute of Molecular Science, Okazaki 444-8585, Japan

³National Institute for Materials Science, Tsukuba 305-0047, Japan

When ferromagnetic transition metals (TMs) are deposited on the Rashba-type spin-orbit coupled surface, novel properties such as perpendicular magnetic anisotropy (PMA) are emerged at the interfaces, which are derived from the symmetry broken spin-orbit effects. The gold Au (111) surfaces have been investigated extensively by means of scanning tunneling microscopy and angle-resolved photoemission spectroscopy (ARPES) because this surface exhibits the large Rashba-type spin-orbit splitting. Large spin-orbit interaction in the heavy element of gold provides the wide varieties for the topological physics and spin-orbit coupled sciences at the surfaces and interfaces. The Rashba splitting of 110 meV in Au (111) surface was reported firstly by LaShell *et al.* [1]. Recently, the interfaces between Au(111) and other heavy elements such as Bi or Ag have been extensively investigated [2,3]. Here, we focus on the interfaces between ferromagnetic materials and Au(111) interfaces because the thin Fe layers on the heavy elements are expected to exhibit the PMA induced by the Rashba-type spin-orbit interaction.

The spin-orbit coupling between the ferromagnetic 3d TMs Fe or Co and 5d heavy TM elements of non-ferromagnetic materials such as Pt and Au has been utilized for the PMA through the proximity at the interfaces. It is believed that the future researches concerning not only spins but also orbitals are recognized as the *spin-orbitronics*. Therefore, to clarify the origin of the PMA at these interfaces is a crucial role. The relationship between Au (111) Rashba-type spin-orbit interaction and PMA in 3d TMs has not been clarified explicitly. In order to investigate the orbital-resolved states in the Fe films showing the PMA, ARPES at the interfaces becomes powerful techniques through the photon-energy and polarization dependences in each 3d orbital. By using ARPES, we aim to understand the orbital-resolved electronic structures at the magnetic interfaces on the Rashba-type Au (111) surface in order to develop the researches of novel PMA using spin-orbit coupled interfaces.

We prepared the clean Au (111) surface for the Fe deposition. The commercialized single-crystalline 100-nm-thick Au (111) films on Mica were used. At the BL5U in UVSOR, we repeated the Ar-ion sputtering at 1-2 kV accelerating voltage and subsequent annealing at 400 °C under the high vacuum conditions. After the sample preparation, the Fe layer

was deposited at room temperature and then annealed. By *in-situ* transferring the samples into the ARPES chamber, we performed ARPES at 10 K using the photon energies of 45 and 120 eV because of the large cross-section of Au (111) surface states and detections of Fe 3p and Au 4f intensity ratios, respectively.

Figure 1 displays the Fe deposition dependence on Au (111). As shown in Fig. 1a, the intensity ratio between Fe 3p and Au 4f peaks systematically changes. The Au (111) surface clearly exhibits the Rashba-type surface states (Fig. 1c). The Fe 3d states appear near the Fermi level (E_F) and the surface states disappear as shown in Fig. 1d. As shown in Fig. 1b, with increasing the Fe layer thickness, spectral line shapes cannot be explained by the overlap between Fe and Au, suggesting that the chemical bonding at the interface is modulated from the Au (111) surface and Rashba-type spin-orbit interaction affects to the Fe layer. Therefore, the interfacial chemical reaction between Fe and Au brings the novel properties on the ultrathin Fe electronic structures.

We acknowledge Dr. S. Ideta in IMS for technical supports of data analyses. This work was in part supported by KAKENHI Kiban(S) project.

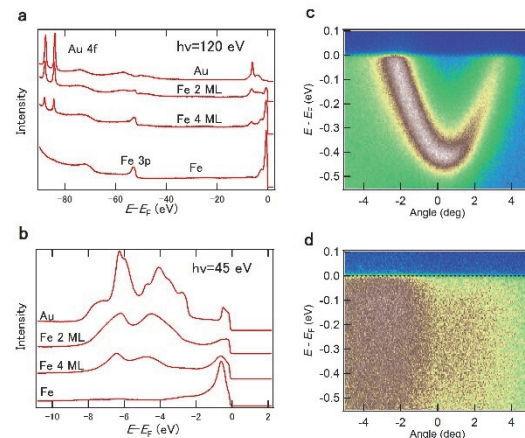


Fig. 1. Photoemission spectra for various Fe deposited layers. **a.** Angle-integrated wide-range spectra taken at 120 eV. **b.** valence-band spectra taken at 45 eV. **c.** ARPES near E_F in Au surface taken at 45 eV. **d.** ARPES near E_F after 2 ML Fe deposition taken at 45 eV.

[1] S. LaShell *et al.*, Phys. Rev. Lett. **77** (1996) 3419.

[2] C. Tusche *et al.*, Ultramicroscopy **159** (2015) 620.

[3] B. Yan *et al.*, Nature Commun. **6** (2015) 10167.

*e-mail: jun@chem.s.u-tokyo.ac.jp

BL5U

Photoelectron Angular Distribution Maps of Perfluoropentacene on Ag (111)

T. Yamaguchi^{1,2}, S. Ouchi³, M. Meissner¹, T. Ueba^{1,2}, R. Shiraishi^{1,2}, S. Ideta^{1,4}, K. Tanaka^{1,4}
and S. Kera^{1,2,3}

¹School of Physical Sciences, The Graduate University for Advanced Studies (SOKENDAI), Okazaki 444-8585

²Department of Photo-Molecular Science, Institute for Molecular Science, Okazaki 444-8585, Japan

³Graduate School of Engineering, Chiba University, Chiba 263-8522, Japan

⁴UVSOR Synchrotron Facility, Institute for Molecular Science, Okazaki 444-8585, Japan

The interface between a molecular semiconductor and a metal greatly affects the electronic properties of the molecular film and it is thus of great importance to fundamentally study the large variety of effects taking place at such an interface. Photoelectron angular distribution (PAD) maps generated from angle-resolved ultraviolet photoemission spectroscopy (ARUPS) provide insight into the orbital shapes of adsorbed molecules. By comparing experiments with theoretical data allows us to discuss the origin of modifications of orbitals and the implications for the electronic properties of the film. Here, we aimed to test the suitability of BL5U with the deflector mode for this purpose, using monolayers of perfluoropentacene (PFP) adsorbed on Ag(111).

We prepared monolayers of PFP on Ag(111) by annealing slightly thicker films at 130 °C for 10 min. These samples were then measured at room temperature as well as at 5 K, using different photon energies of 60 eV and 120 eV. An exemplary PAD map is shown in Fig. 1a for a sample that is tilted away from the normal-emission geometry, such that the Γ point is outside the upper left corner of the image. The arc-like feature in the center belongs to the Ag sp-band, whereas the feature in the center belongs to the second-highest occupied molecular orbital (HOMO^{-1}). The $\bar{\Gamma}\bar{K}$ direction of Ag(111) is aligned horizontally.

By probing the photoelectrons at different binding energies, we generated three-dimensional energy-versus-angle data, enabling us to discuss spectroscopic details and dispersion behavior of the films. Fig. 1b shows a cut through that data in the direction indicated by the red line in panel a. The HOMO and HOMO^{-1} are marked by horizontal lines.

Building on experiences from a previous beamtime at BL5U, we aimed to reduce film damages due to the intense beam by measuring during single-bunch operation. Obviously, however, there are low-energy shoulders next to both the HOMO and HOMO^{-1} , which is a typical indication of molecules broken up by the irradiation. Moreover, the field of view (FoV) of this setup is quite limited compared to the angular dimensions of typical molecular orbitals. It is sufficient to discuss fine features of individual orbital lobes. However, a stitching of images taken under different rotation/tilting angles of the sample in order to obtain a more complete PAD map is hardly possible or meaningful due to the changing beam incidence angle.

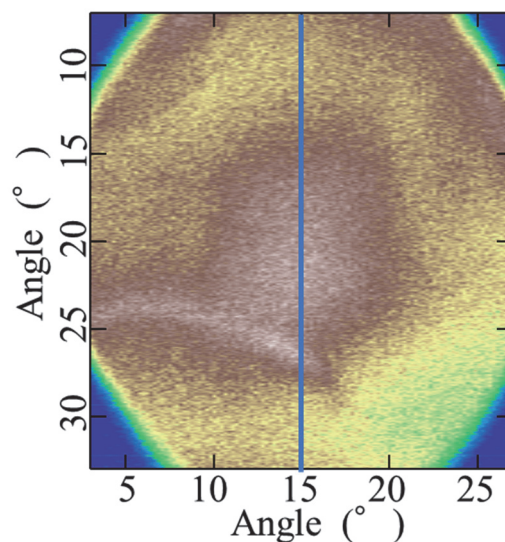


Fig. 1. Angle-resolved photoelectron map of HOMO^{-1} for monolayer PFP on Ag(111) at $h\nu= 60$ eV. The blue line marks the cut direction for the image in Fig. 2.

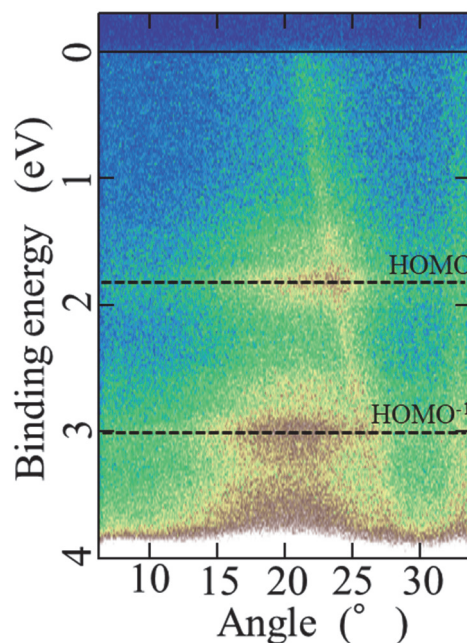


Fig. 2. Binding energy versus emission angle in the direction highlighted in Fig. 1, overlaid by the horizontally integrated energy distribution curve. The HOMO and HOMO^{-1} of PFP are marked by horizontal dashed lines.

BL5U, BL7U

Electronic Structure of Mn and Te Deposited Bi_2Te_3 : A New Magnetic Topological Heterostructure

 K. Yokoyama¹, Y. Okuyama¹, S. Ideta², K. Tanaka² and T. Hirahara¹
¹Department of Physics, Tokyo Institute of Technology, Tokyo 152-8551, Japan

²UVSOR Synchrotron Facility, Institute for Molecular Science, Okazaki 444-8585, Japan

Topological insulators (TI) are extensively studied recently due to its peculiar properties [1]. The Dirac-cone surface states of TI are protected by time-reversal symmetry (TRS) and backscattering among these surface states is prohibited. But when TRS is broken by application of a magnetic field or incorporating magnetic materials, a gap opening in the Dirac cone is expected and an intriguing phase called the quantum anomalous Hall state can be realized [2]. This phase is expected to show even more exotic phenomena such as the topological magnetoelectric effect. To realize such state, two types of sample fabrication techniques have been employed up to now: (1) magnetic doping while growing the single crystal or thin film of TI [3], and (2) magnetic impurity deposition on the surface of TI [4]. While method (1) was successful and showed evidence of the TRS violation, no one has succeeded using method (2), which should be a more direct way to examine the interaction between the topological surface states and magnetism. Recently, we have succeeded in inducing a gap in the TI Dirac surface states by a new method called ‘magnetic extension’ [5]. An ordered Mn layer was incorporated into the topmost quintuple layer of a prototypical TI, Bi_2Se_3 by Mn and Se deposition and a $\text{MnBi}_2\text{Se}_4/\text{Bi}_2\text{Se}_3$ heterostructure was formed. Due to the large wave function overlap between the Dirac cone and the ferromagnetic Mn layer, a large gap of 85 meV was observed [6].

In the present work, we have tried to employ magnetic extension to break the TRS in another prototypical TI, Bi_2Te_3 . We deposited Mn and Te on Bi_2Te_3 and measured its electronic structure. Figures 1 (a) and (b) show the band dispersion of the surface states of the pristine Bi_2Te_3 and the sample with Mn and Te deposited on top measured at 30 K ($h\nu = 8$ eV). The Dirac-cone surface states are massless in (a) with no gap. On the other hand, one can find a clear gap of ~ 70 meV at the Dirac point in (b) as indicated by the energy distribution curve, meaning that it has turned into a massive Dirac cone. This result shows that we have successfully induced TRS breaking in the surface states of Bi_2Te_3 . However, comparison with *ab initio* calculations [5] showed that the formed structure is not $\text{MnBi}_2\text{Te}_4/\text{Bi}_2\text{Te}_3$ and a structural study is under way to determine the real crystal structure of the system.

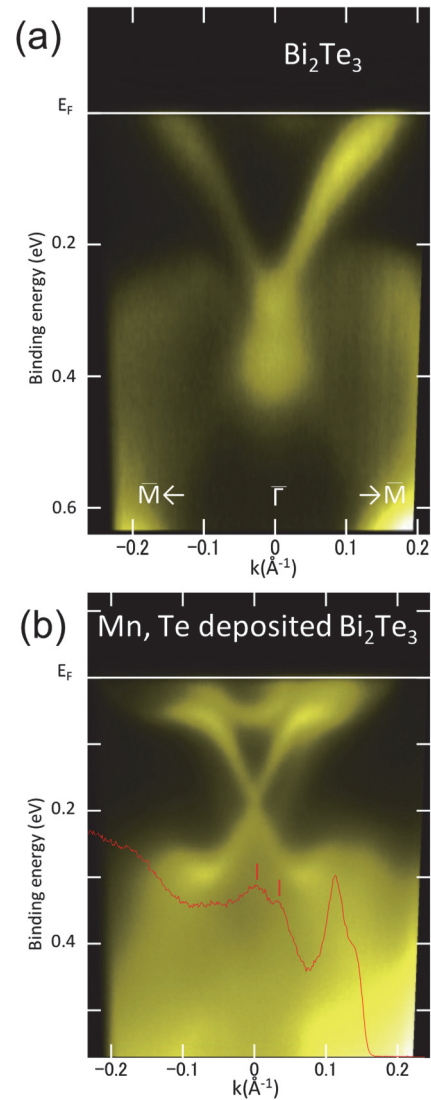


Fig. 1. The band dispersion of Bi_2Te_3 (a), and that with Mn and Te deposition (b), respectively, measured at 30 K with $h\nu = 8$ eV photons of *p*-polarization.

[1] M. Hasan and C. Kane, *Rev. Mod. Phys.* **82** (2010) 3045.

[2] X.-L. Qi and S.-C. Zhang, *Rev. Mod. Phys.* **83** (2011) 1057.

[3] For example, C. Z. Chang *et al.*, *Science* **340** (2013) 167.

[4] For example, M. Ye *et al.*, *Phys. Rev. B* **85** (2012) 205317.

[5] M. Otrikov *et al.*, *2D Mater.* **4** (2017) 025082.

[6] T. Hirahara *et al.*, *Nano Letters* **17** (2017) 3493.

BL5B

Optical Properties of Amorphous Arsenic Trisulfide

K. Hayashi

Department of Electrical, Electronic and Computer Engineering, Gifu University, Gifu 501-1193, Japan

Amorphous chalcogenide semiconductor materials, such as a-As₂S₃, a-As₂Se₃ and a-Se etc., show a variety of photo-induced phenomena. These materials are expected as materials for optoelectronic devices. A lot of work have been done on the photo-induced phenomena of these amorphous semiconductor materials and various mechanisms have been proposed for these photo-induced phenomena [1-3]. However, the details of the mechanisms are still unknown. For device applications, it is necessary to sufficiently understand the fundamental properties of these materials. The interest has been attracted for the change of the optical properties in the energy region of the visible light. We are interesting for the changes of the optical properties in the higher energy region. To our knowledge, little attention has been given to photo-induced changes at the vacuum ultra-violet (VUV) absorption spectrum. In previous reports, we reported the photo-induced change at VUV transmission spectra of as-deposited evaporated amorphous As₂Se₃ thin films [4]. In this report, we measure the VUV transmission spectra on as-deposited evaporated amorphous As₂S₃ thin films.

Samples used for the measurement of the VUV transmission spectra were amorphous As₂S₃ thin films prepared onto aluminum thin films by conventional evaporation technique. Typical thickness of the amorphous film and the aluminum film were around 200 nm and 100 nm, respectively. The measurements were carried out at room temperature at the BL5B of the UVSOR Synchrotron Facility of the Institute for Molecular Science. And the spectrum was measured by using the silicon photodiode as a detector. Two pinholes of 1.5 mm in a diameter were inserted between the monochromator and sample to remove stray light. The intensity of the VUV light was monitored by measuring the total photoelectron yield of a gold mesh.

Figure 1 shows the transmission spectra of as-deposited a-As₂S₃ thin film at room temperature in the wavelength range (a) 7.5-8.9nm and (b) 25-30nm. Several peaks were observed at this wavelength range. The absorption peaks around 7.7nm correspond to the 2*p* core level of S atom. Other peaks correspond to the 3*p* and 3*d* core level of As atom. The broad structures observed in the absorption spectra. The origin of each component is not clear now. I would like to clarify the origin of each component in the future. Further analysis of these spectra is now in progress. We pay attention to the photo-induced effects near this wavelength range. We now are investigating photo-induced change on these spectra. The detailed experiments and analysis will be done in the next step.

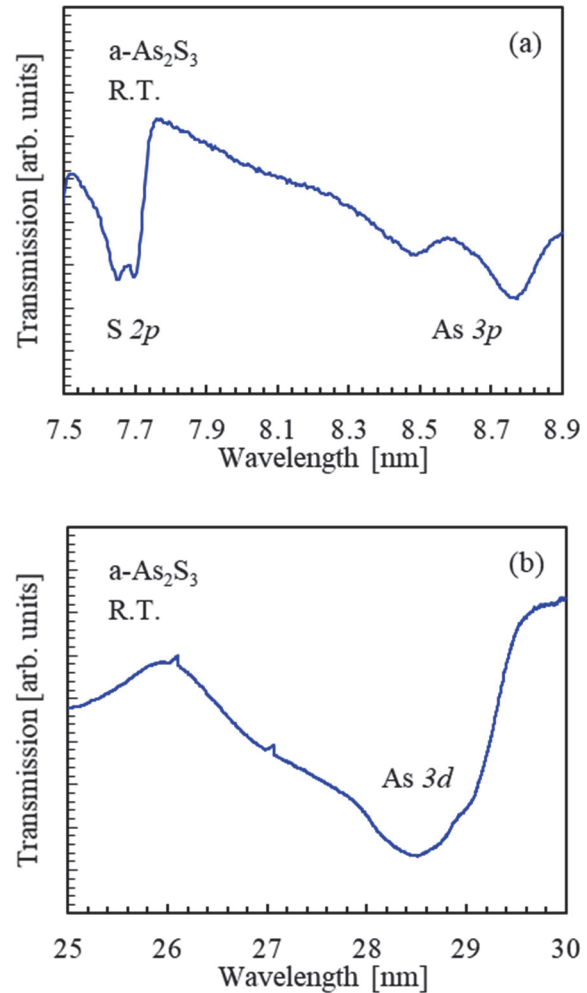


Fig. 1. The transmission spectra of as-deposited a-As₂S₃ thin film in the wavelength range (a) 7.5-8.9nm and (b) 25-30nm.

- [1] K. Tanaka, *Rev. Solid State Sci.*, **4** (1990) 641.
- [2] K. Shimakawa, A. Kolobov and S. R. Elliott, *Adv. Phys.*, **44** (1995) 475.
- [3] K. Tanaka, *Encyclopedia of Nanoscience and Nanotechnology*, **7** (2004) 629.
- [4] K. Hayashi, *UVSOR Activity Report 2014* **42** (2015) 134.

BL6U

Band Engineering of Silicene-Ge Alloy

A. Fleurence¹, T. Yonezawa¹, H. Yamane², N. Kosugi² and Y. Yamada-Takamura¹

¹*School of Materials Science, Japan Advanced Institute of Science and Technology, Nomi 923-1292, Japan*

²*Institute for Molecular Science, Okazaki 444-8585, Japan*

Alloying plays an important role for applications as it gives solution to tune the properties of materials. For instance, the band gap can be tuned in bulk SiGe alloy by means of the concentration of Ge atoms [1].

Silicene is a graphene-like buckled honeycomb structure made of silicon atoms featuring π bands at the K points of its Brillouin zone [2]. As a two-dimensional material, silicene is of high interest for Si-based nanoelectronics.

Silicene only exists in epitaxial forms. Among them, epitaxial silicene on ZrB₂ thin films grown on Si(111) has the particularity to form in a spontaneous and self-terminating way by segregation of Si atoms from the silicon substrate [3]. Epitaxial silicene adopts a silicene- $(\sqrt{3}\times\sqrt{3})$ reconstructed unit cell in which 5 Si atoms are in the same plane and a single atom is protruding. This silicene is semiconducting as a 350 meV-wide gap is opened in the Dirac cones [3].

We demonstrated by means of scanning tunneling microscopy at our home laboratory that the deposition of germanium on silicene can give rise to a silicene-Ge alloy resulting from the incorporation of Ge atoms into the silicene lattice [4].

The experiments done at the BL6U of UVSOR were aimed at determining the evolution of the band structure of this silicene-Ge alloy with the concentration of Ge atoms.

Water-cooled mini K-cell, which we used for the experiments in our home-based setup, was installed in the preparation chamber of the end station for evaporating Ge. Epitaxial silicene samples were prepared on-site by annealing ZrB₂/Si(111) samples at 800 °C under ultrahigh vacuum [2]. Ge growths were realized with a substrate temperature of 350 °C. All photoemission spectra were recorded at 15 K.

The core-level of Fig. 1(a) shows a single Ge 3d component which indicates that the Ge atoms are incorporated in a unique site in the silicene lattice. The saturation of this peak for a Ge coverage of about 1/6 monolayer (ML) silicene points out that Ge atoms occupy the protruding sites in the silicene lattice. More importantly, a clear effect of the Ge atoms on the band structure was found as the top of the valence band shifts up monotonously with the concentration. Figs. 1(c) and (d) compare angle-resolved photoemission (ARPES) spectra of pristine silicene and of silicene-Ge alloy at saturation. In the latter, the top of the band is shifted by 160 meV above that of pristine silicene.

These experiments provide an experimental demonstration of the possibility of band gap engineering in SiGe two-dimensional materials as for their bulk counterparts.

This work was supported by the Joint Studies

Program (No. 206, 2017-2018) of the Institute for Molecular Science.

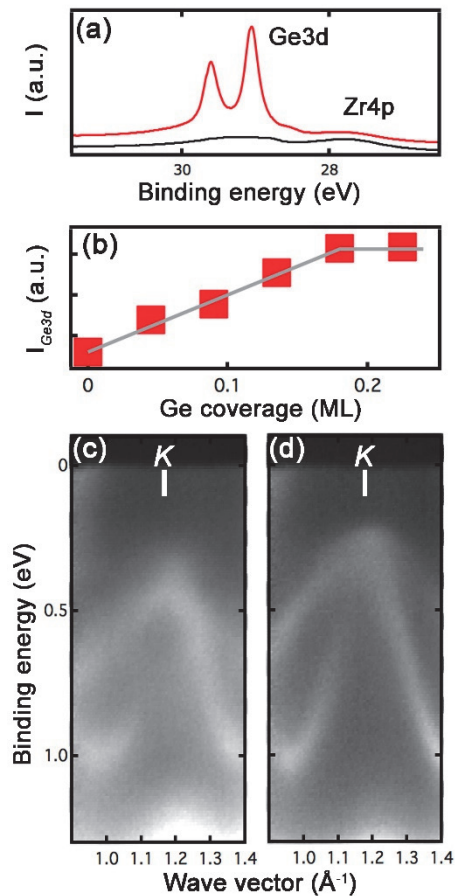


Fig. 1. (a): Core-level spectra ($h\nu=80$ eV) in the Zr 4p and Ge 3d region before and after deposition of 0.04 ML Ge on silicene. (b): Evolution of the Ge3d peak with the Ge coverage. (c) and (d) ARPES spectra ($h\nu=45$ eV) of pristine silicene and after deposition of 0.18 ML Ge.

[1] J. C. Bean, Proc. IEEE **80** (1992) 571.

[2] K. Takeda and K. Shiraiishi, Phys. Rev. B **50** (1994) 14916.

[3] A. Fleurence *et al.*, Phys. Rev. Lett. **108** (2012) 245501.

[4] Y. Awatani, *et al.*, Bulletin of the American Physical Society, 2016 March Meeting, T1.307.

BL6U

Self-Encapsulation of Epitaxial Silicene on ZrB₂ under a h-BN Monolayer

A. Fleurence¹, T. Yonezawa¹, M. P. de Jong², M. W. Ochapski², H. Yamane³,
N. Kosugi³ and Y. Yamada-Takamura¹

¹*School of Materials Science, Japan Advanced Institute of Science and Technology, Nomi 923-1292, Japan*

²*MESA+ Institute for Nanotechnology, University of Twente, 7500 AE Enschede, The Netherlands*

³*Institute for Molecular Science, Okazaki 444-8585, Japan*

Silicene, as a graphene-like silicon two-dimensional material has great expectation to give solution to scale down further the Si-based nanotechnologies. Even if a first transistor based on silicene could be fabricated [1], its quick oxidation in air indicates that silicene encapsulation is a crucial point to address for processing it routinely and fabricate reliable devices.

Silicene only exists in epitaxial forms. Among them, epitaxial silicene on ZrB₂ thin films grown on Si(111) has the particularity to form in a spontaneous and self-terminating way by the segregation of Si atoms from the silicon substrate [2].

It is also possible to fabricate a monocrystalline h-BN single layer covering the entire ZrB₂ thin film surface [3]. The deposition of silicon on this h-BN/ZrB₂ surface gives rise to a surface structure resembling that of epitaxial silicene. Si2*p* core-level and band structure, indicate that a silicene layer similar to that observed on bare ZrB₂ surface intercalates between the ZrB₂ thin film and the h-BN layer.

The purpose of these experiments at BL6U was to determine whether the h-BN layer is capable of preventing the oxidation of silicene.

Epitaxial silicene and oxide-free h-BN samples were prepared on-site by annealing at 800 °C under ultrahigh vacuum ZrB₂/Si(111) [2] and h-BN/ZrB₂/Si(111) samples we elaborated at our home laboratory. Silicon was evaporated by heating a piece of silicon in front of the h-BN/ZrB₂ surface held at room temperature (RT). Core-level spectra in the Si2*p* region were recorded with a surface-sensitive photon energy of $h\nu=130$ eV at RT.

The comparison of the core-level spectra of pristine silicene before and after a 5 min exposure to air (Figs. 1(a) and (b)) shows that the typical spectrum of silicene has turned into a Si oxide peak, which confirms the destruction of silicene in air. The spectrum recorded after deposition of silicon on h-BN/ZrB₂ is visible in Fig. 1(c). It differs from that of Fig. 1(a) due to an excess of silicon forming amorphous islands. Most importantly, after exposure to air with duration up to 60 min (Figs. 1(d)-(e)), the silicene component remains while a small oxide peak appears. It can be noticed that the line shape of the silicene component now more closely resembles that of pristine silicene, which indicates that the silicon oxide peak corresponds to the excess of Si.

The fact that the spontaneously encapsulated silicene survived an exposure long enough to allow for taking silicene in air opens the way to the possibility of processing silicene *ex-situ* in a controlled

environment.

This work was supported by the Joint Studies Program (No. 206, 2017-2018) of the Institute for Molecular Science.

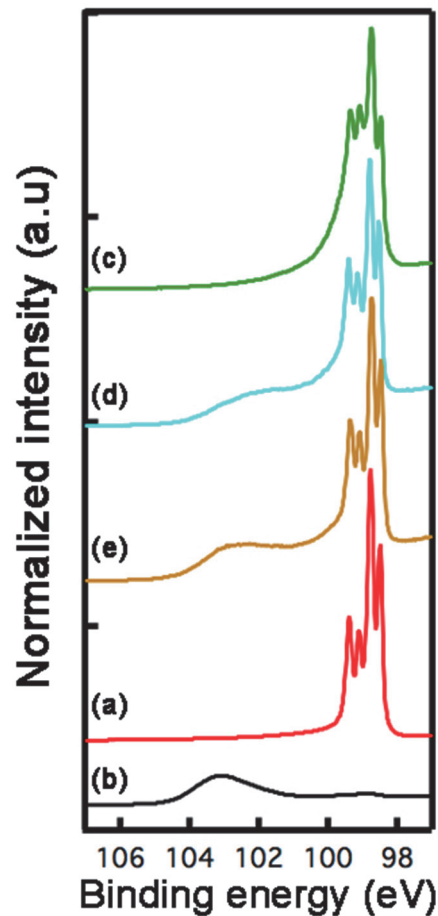


Fig. 1. (a) and (b): Normalized core-level spectra ($h\nu=130$ eV) in the Si2*p* region before and after a 5 min exposure to air of unencapsulated silicene. (c): Core-level spectrum of intercalated silicene. (d) and (e): Core-level spectra of intercalated silicene recorded after 5 and 60 min exposures to air.

[1] L. Tao *et al.*, Nature Nanotech. **10** (2015) 227.

[2] A. Fleurence *et al.*, Phys. Rev. Lett. **108** (2012) 245501.

[3] Z.-T. Wang *et al.*, J. Appl. Phys. **100** (2006) 033506.

BL6U

Thin-film Structure Depending on the Sulfur Substitution of Phenanthro-dithiophene Isomers

S. Ouchi¹, C. Numata¹, T. Yamaguchi^{2,3}, M. Meissner³, T. Ueba^{2,3}, H. Yamane^{2,3},
N. Kosugi^{2,3}, H. Yoshida¹, K. Hyodo⁴, Y. Nishihara⁴ and S. Kera^{1,2,3}

¹ Graduate School of Engineering, Chiba University, Chiba 263-8522, Japan

² Institute for Molecular Science, Okazaki 444-8585, Japan

³ The Graduate University for Advanced Studies (SOKENDAI), Okazaki 444-8585, Japan

⁴ Research Institute for Interdisciplinary Science, Okayama University, Okayama 700-8530, Japan

Even a subtle difference of intermolecular interaction can impose a large change in molecular ordering and electronic properties at organic semiconductor/metal interface. We examined two picene analogues, phenanthro-dithiophene isomers (PDT1 and PDT2), where the sulfur atoms are substituted differently as shown in Fig.1. We investigated the effect of the isomeric structure on the thin film structure as well as the electronic state.

The Au(110) substrate was cleaned by the repeated cycles of the Ar-ion sputtering and the subsequent annealing at 873 K. The monolayer (ML) films were prepared by the vacuum deposition onto the clean Au(110) surface at 300 K. The deposition rate was 0.05 nm/min. After depositing the ML, the PDT1 and PDT2 samples were annealed at 373 K.

Figure 2 shows the LEED images of PDT1 and PDT2 MLs on Au(110). Before the annealing, no sharp spots appear, while the sharp spots appear after the annealing for the PDT1 film. On the other hand, exhibits the stripe pattern for both as-grown and annealed films. The observed LEED images indicate that the PDT1 molecules on Au(110) form a long-range ordered structure in two directions, while the PDT2 molecules on Au(110) form it in only one-dimensional ordered structure. This difference is caused by a different intermolecular interaction assisted by the larger permanent dipole of PDT1.

Figure 3 shows the comparison of XPS spectra of the MLs of PDT1 and PDT2 ($h\nu = 335$ eV). The upper panel (a) show the spectra before the annealing and the bottom panel (b) show the one after the annealing. While no differences are discernible between PDT1 and PDT2 for the as-grown film, two changes are clearly observed in the spectra upon the annealing. First, the binding energy of PDT1 is smaller than that of PDT2 by about 100 meV in S2p spectra. Second, comparing C1s spectra, we also observed the binding energy shift of 30 meV and the different line shapes between PDT1 and PDT2. The observed XPS spectra indicate that the interaction between gold and sulfur of the PDT1 is stronger than that of the PDT2.

Understanding the relationship between the substitution position of the sulfur and the thin film structure more precisely, we would discuss the impacts of the thin film structure on the electronic states.



Fig. 1 Molecular structures of PDT1 (left) and PDT2 (right).

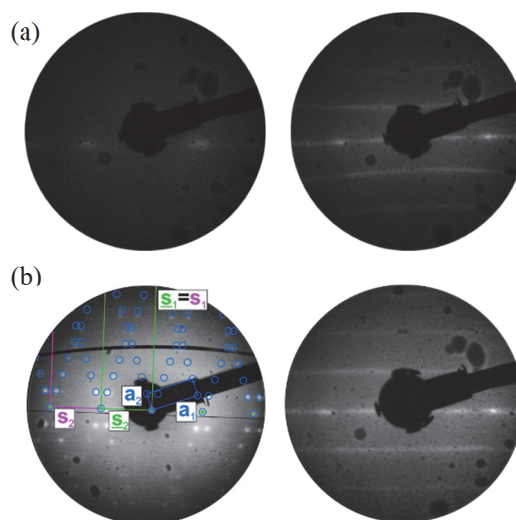


Fig. 2 Comparison of LEED images of PDT1 (left) and PDT2 (right). (a) before the annealing, (b) after the annealing.

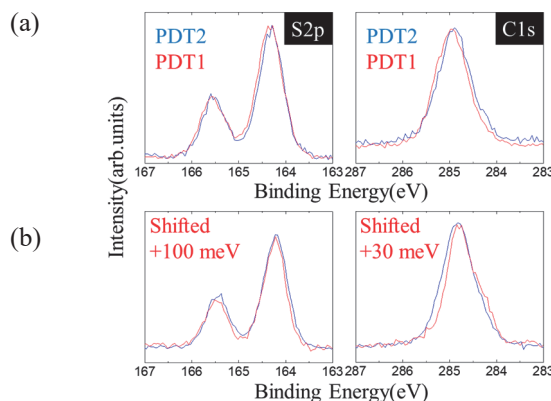


Fig. 3 Comparison of XPS spectra of PDT1 (red) and PDT2 (blue) MLs on Au(110). (a) before the annealing, (b) after the annealing (S2p and C1s peaks are aligned by 100 meV and 30 meV, respectively).

BL6U

Effects of Surface Adsorbates on the Electronic Structure of Excitonic Insulator Ta_2NiSe_5

 K. Fukutani¹, R. Stania¹, J. Jung^{1,2}, H. Yamane³, N. Kosugi³ and H. W. Yeom^{1,2}
¹Center for Artificial Low Dimensional Electronic Systems, Institute for Basic Science (IBS), Pohang 37673, Republic of Korea

²Department of Physics, Pohang University of Science and Technology (POSTECH), Pohang 37673, Republic of Korea

³Department of Photo-Molecular Science, Institute for Molecular Science, Okazaki 444-8585, Japan

Bound pairs of conduction band electrons and valence band holes, so-called excitons, can be formed within solids as a meta-stable state induced by external excitations, such as light irradiation. On the other hand, it has also been proposed theoretically for more than half a century that, for narrow-gap semiconductors and semimetals, a finite number of excitons can condense in the ground state to form what is called an excitonic insulator [1, 2]. However, due to number of experimental difficulties, the direct elucidation of such excitonic condensate was revealed only recently [3].

Ta_2NiSe_5 is among the few materials that are proposed to be excitonic insulators, and a number of studies have recently been performed to explore the nature of excitonic phase of this material, including the presence of many-body band gap near the Fermi level [4], band gap tuning by chalcogen substitutions [5], and layer-confined nature of excitonic phases [6].

Our previous studies on Ta_2NiSe_5 , utilizing the low-energy photon source, revealed that some surface adsorbates on this material induce a renormalization of the excitonic band structure. While the small excitonic radii in the surface-normal direction and their, layer-confined nature likely makes it possible for the surface adsorbates to modify the excitonic insulator phase at the topmost surface, the detailed mechanisms by which the renormalization occurs required further investigation.

In our experiments conducted at BL6U at UVSOR, the excitonic insulator phase of Ta_2NiSe_5 was investigated using the angle-resolved photoelectron spectroscopy (ARPES). As shown in Fig. 1(a), the unusual flattening of the topmost valence band is observed, which is believed to be a signature of the excitonic condensate for $T < T_c$. Our ARPES data also reveal the band structure perpendicular to the quasi-one-dimensional atomic chain as shown in Fig. 1(b) indicating small, yet finite inter-atomic chain interactions. Upon adsorption of potassium (K) as surface dopants, the Ta 4f core levels are seen to shift towards higher binding energy by ~ 40 meV (see Fig. 2), indicating that K adsorption results in the electron-doping at the surface. While further investigations, including model calculations, are required to make definite conclusions, the experimental results obtained at BL6U likely indicate the change in the free carrier concentration induced by the surface dopants screens the attractive Coulomb interaction between the

electrons and holes, thereby modifying the binding energy of excitons at condensate.

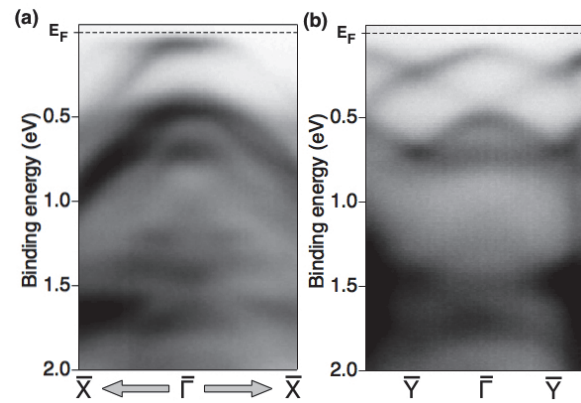


Fig. 1. (a) The ARPES band mapping taken at photon energy of $h\nu = 60$ eV along the Γ -X direction (parallel to the quasi-one-dimensional atomic chain) and (b) along the Γ -Y direction (perpendicular to the atomic chain). The sample temperature was maintained at $T = 40$ K.

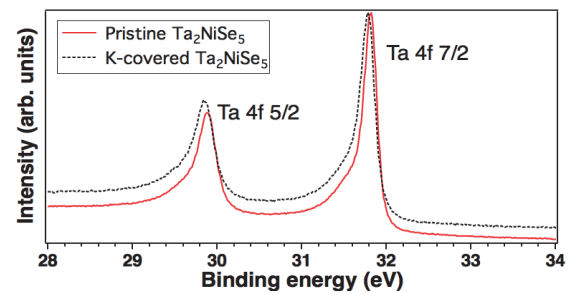


Fig. 2. The evolution of the Ta 4f core level spectra with upon K adsorption, taken at $h\nu = 60$ eV, $T = 40$ K. The both spin-orbit split pair of Ta 4f core levels are seen to move towards the higher binding energy with K adsorption, indicating the n -type doping on the sample surface.

- [1] N. F. Mott, *Phil. Mag.* **6** (1961) 287.
- [2] W. Kohn, *Phys. Rev. Lett.* **19** (1967) 439.
- [3] C. Monney *et al.*, *Phys. Rev. B* **79** (2009) 045116.
- [4] Y. Wakisaka *et al.*, *Phys. Rev. Lett.* **103** (2009) 026402.
- [5] Y. F. Lu *et al.*, *Nat. Commun.* **8** (2017) 1.
- [6] S. Y. Kim *et al.*, *ACS Nano* **10** (2016) 8888.

BL7U

Photoelectron Angular Distribution of Anthradithiophene on Graphite Investigated by Low-energy Angle Resolved Photoelectron Spectroscopy

T. Yamaguchi^{1,2}, M. Meissner², T. Ueba^{1,2}, R. Shiraishi^{1,2}, S. Ideta^{1,3},
K. Tanaka^{1,3} and S. Kera^{1,2}

¹*School of Physical Sciences, The Graduate University for Advanced Studies (SOKENDAI), Okazaki 444-8585*

²*Department of Photo-Molecular Science, Institute for Molecular Science, Okazaki 444-8585, Japan*

³*UVSOR Synchrotron Facility, Institute for Molecular Science, Okazaki 444-8585, Japan*

Ultraviolet photoelectron spectroscopy (UPS) is a very useful technique for studying the electronic structure of surfaces and interfaces. However, UPS with low energy photons is not well understood theoretically and experimentally because of the complicated photoemission process. For instance, resonances excitation between initial states and final states occur which cause unexpected scattering due to the relatively long dwell time of low-energy electrons at the surface/interface (potential trapping in intermediate states) [1]. Moreover, the asymmetric parameter of the photoelectron intensity greatly depends on the photon energy ($h\nu$). In this work, we investigated the photoelectron angular distribution (PAD) of the highest occupied molecular orbital (HOMO) for anthradithiophene (ADT), using low-energy angle-resolved UPS (LE-ARUPS), aiming to improve the understanding of the photoemission process in the low energy region at organic-metal interfaces.

Highly oriented pyrolytic graphite (HOPG) as the substrate was cleaned by annealing at 600 K for 2 h. An ADT molecule film of 5 Å was deposited on the HOPG at room temperature in a custom UHV chamber designed for organic layer deposition.

Figures 1 (a) and (c) show a LE-ARUPS intensity

map and energy distribution curves, respectively, taken at $h\nu = 21$ eV. The HOMO peak was observed at 1.40 eV and around -1.5 Å⁻¹ in Fig. 1 (a). Around the Γ point, there is no momentum dependence of the HOMO intensity. This is a typical PAD of the HOMO of the π -conjugated, planar molecules in a flat-lying orientation.

Figures 1 (b) and (d) show a LE-ARUPS intensity map and energy distribution curves, respectively, taken at 11 eV. It is impossible to observe the main HOMO-intensity lobe by 11 eV due to the low kinetic energy of the photoelectrons. Even though the photons come from right side of the image, the HOMO intensity at 0.5 Å⁻¹ is 3 times stronger than that at -0.5 Å⁻¹. Moreover, a sudden change of intensity occurs at the Γ point. The direction of the p-polarized incident beam normally causes the opposite intensity distribution as found in Fig. 1 (a).

We clearly observed an interesting difference of PAD between $h\nu = 21$ eV and 11 eV which will be caused by non-trivial multi-particle events in the photoemission. The multiple scattering theory will be helpful to understand the origin of the PAD, hence to reveal the modification of the molecular orbital upon weak interactions.

[1] S. Tanaka *et al.*, *Sci. Rep.* **3** (2013) 3031.

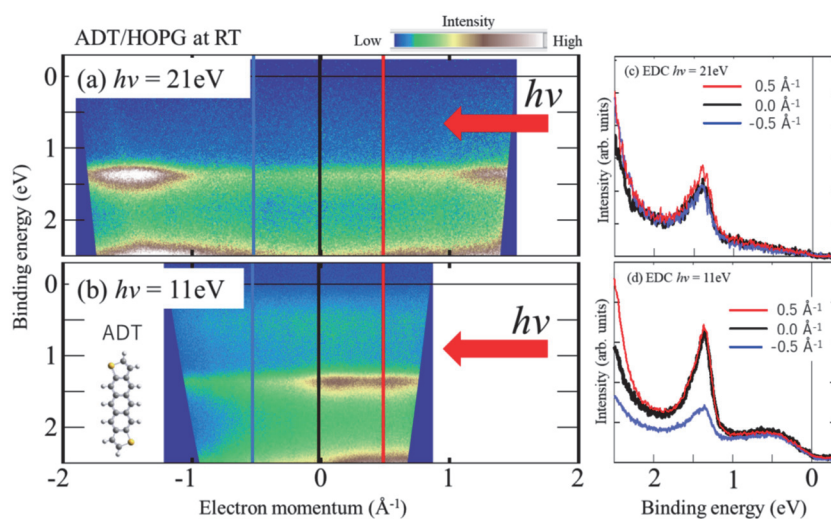
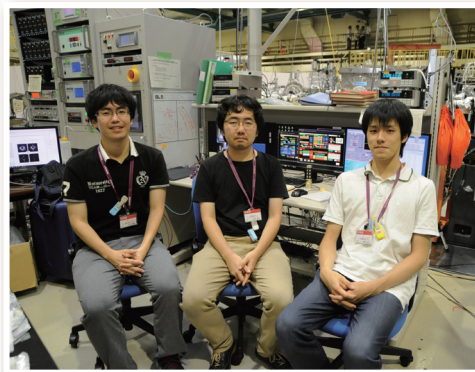
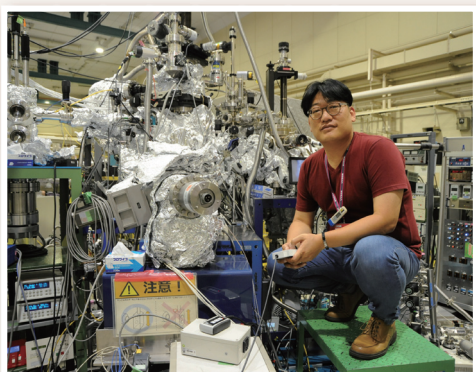
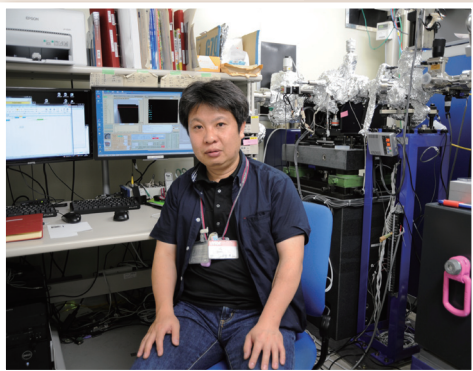
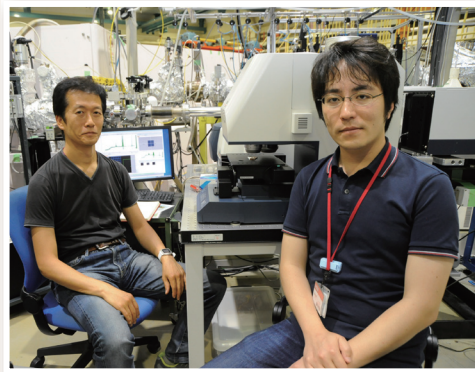
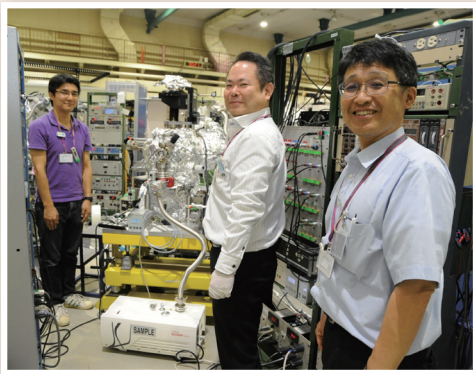
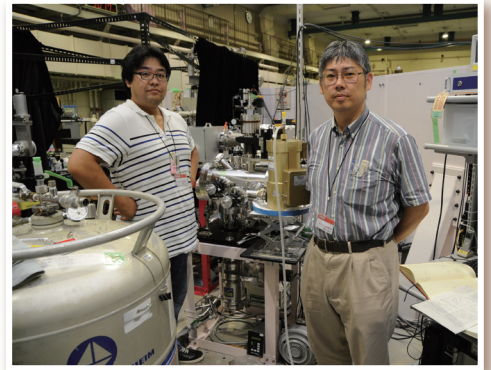
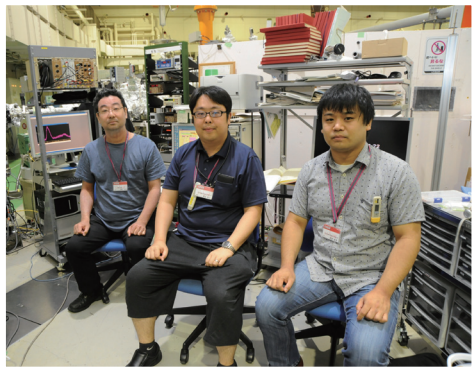
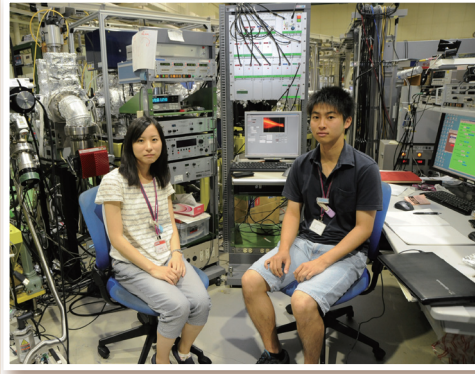
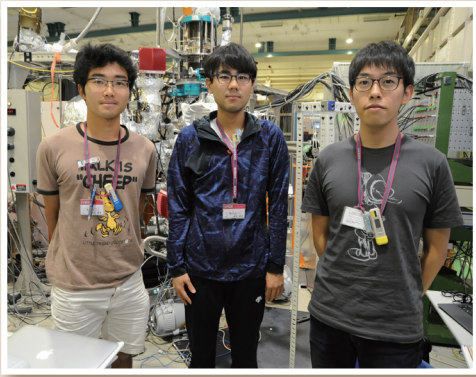


Fig. 1. LE-ARUPS intensity map for ADT/HOPG taken at room temperature using $h\nu = 21$ eV (a) and 11 eV (c). Both images were prepared by combining 8 and 7 images taken every 12° . Energy distribution curves at -0.5 Å⁻¹, 0.0 Å⁻¹ and 0.5 Å⁻¹ taken for $h\nu = 21$ eV (b) and 11 eV (d). Red arrows represent the incident light direction. The structure of the ADT molecule is shown as an inset in (b).

UVSOR User 5



UVSOR User 6

